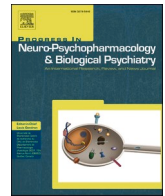




Contents lists available at ScienceDirect

Progress in Neuropsychopharmacology & Biological Psychiatry

journal homepage: www.elsevier.com/locate/pnp

Dynamic functional connectivity in schizophrenia and bipolar disorder: A review of the evidence and associations with psychopathological features

Giulia Cattarinussi^{a,b}, Annabella Di Giorgio^c, Federica Moretti^d, Emi Bondi^c,
Fabio Sambataro^{a,b,*}

^a Department of Neuroscience (DNS), University of Padova, Italy

^b Padova Neuroscience Center, University of Padova, Italy

^c Department of Mental Health and Addictions, ASST Papa Giovanni XXIII, Bergamo, Italy

^d Department of Medicine and Surgery, University of Milan Bicocca, Milan, Italy

ARTICLE INFO

Keywords:

Dynamic functional connectivity
ICA
Dynamic fluidity
Schizophrenia
Bipolar disorder
Psychosis
Psychopathology

ABSTRACT

Alterations of functional network connectivity have been implicated in the pathophysiology of schizophrenia (SCZ) and bipolar disorder (BD). Recent studies also suggest that the temporal dynamics of functional connectivity (dFC) can be altered in these disorders. Here, we summarized the existing literature on dFC in SCZ and BD, and their association with psychopathological and cognitive features. We systematically searched PubMed, Web of Science, and Scopus for studies investigating dFC in SCZ and BD and identified 77 studies. Our findings support a general model of dysconnectivity of dFC in SCZ, whereas a heterogeneous picture arose in BD. Although dFC alterations are more severe and widespread in SCZ compared to BD, dysfunctions of a triple network system underlying goal-directed behavior and sensory-motor networks were present in both disorders. Furthermore, in SCZ, positive and negative symptoms were associated with abnormal dFC.

Implications for understanding the pathophysiology of disorders, the role of neurotransmitters, and treatments on dFC are discussed. The lack of standards for dFC metrics, replication studies, and the use of small samples represent major limitations for the field.

1. Introduction

Schizophrenia (SCZ) and bipolar disorder (BD) are severe psychiatric disorders that share a significant overlap in many features, including genetic susceptibility (Lee et al., 2013a; Smoller et al., 2013) and clinical manifestations (Lee et al., 2015). Interestingly, both disorders have been associated with neural changes, mainly involving the fronto-thalamo-striatal and limbic regions (Cattarinussi et al., 2022; Chen et al., 2011; Leroy et al., 2020; Minzenberg et al., 2009; Wu and Jiang, 2020). Studies using functional magnetic resonance imaging (fMRI) in these disorders have found altered functional connectivity also at rest (rs-fMRI), suggesting a role for intrinsic alterations of brain wiring (Lee et al., 2013b). At rest, several regions of the brain show synchronous low-frequency oscillations of the fMRI signal (Fransson, 2005) that suggest a high level of functional coupling or functional connectivity (FC) between them (Menon, 2011; Raichle, 2011; Smith et al., 2009). Importantly, these sets of connected areas, referred to as resting-state networks, show

correspondence with brain networks recruited during the performance of a goal-directed task (Biswal et al., 1997).

Alterations in FC of resting-state networks, particularly the default mode network (DMN), the salience network (SAL), and the executive network (EXE), have been reported in association with several clinical features both SCZ and BD (Hare et al., 2019a; Lee et al., 2018; Menon, 2019; Sambataro et al., 2021a; Whitfield-Gabrieli and Ford, 2012). According to the “triple network” model (Menon, 2011), these networks interact to support cognition, affective functions, and goal-directed behaviors. In particular, the EXE is active in high-order cognition, the DMN is temporally anti-correlated with the EXE and is thought to contribute to vigilance, rumination, self-processing, and learning (Buckner et al., 2008), and the SAL mediates the switching between these networks (Menon, 2011). In addition to these, sensorimotor (SM), visual (VIS), auditory (AUD), language, emotional, and basal ganglia networks have been consistently described at rest in healthy and neuropsychiatric samples (Jimenez et al., 2019; O’Donoghue et al., 2017).

* Corresponding author at: Department of Neuroscience (DNS), Padova Neuroscience Center (PNC), University of Padova, Azienda Ospedaliera di Padova, Via Giustiniani, 2, I-35128 Padua, Italy.

E-mail address: fabio.sambataro@unipd.it (F. Sambataro).

<https://doi.org/10.1016/j.pnpbp.2023.110827>

Received 10 January 2023; Received in revised form 5 June 2023; Accepted 10 July 2023

Available online 18 July 2023

0278-5846/© 2023 The Authors. Published by Elsevier Inc. This is an open access article under the CC BY license (<http://creativecommons.org/licenses/by/4.0/>).

Early resting state studies were based on the assumption that the FC had spatial and temporal stationarity, thus supporting the notion that the average FC could have been representative of the connectivity of the brain. However, brain activity changes dynamically depending on demands, e.g., sleep, sedation, tasks, etc. (Bharath et al., 2017; Harvey et al., 2011), and this also holds for rest, where multiple mental activities can occur (Allen et al., 2014). Therefore, while studies operating under the assumption of stationarity have helped to identify rs-fMRI networks, they have not been able to capture their complex dynamic changes (Hutchison et al., 2013). Accordingly, it has been proposed that the study of time-varying aspects of FC, the so-called dynamic functional connectivity (dFC), may provide greater insight into the properties of brain networks (Allen et al., 2014; Hutchison et al., 2013).

Several measures can be used to characterize the properties of dFC, including functional connectivity strength (FCS), which is a measure of dynamic connectivity calculated as the time-varying sum of connections between a brain voxel and all other voxels and describes the magnitude of signal coupling between brain regions or networks over time in a specific state (Yu et al., 2013). Additionally, measures of stability and predictability of dFC, such as variability, flexibility, entropy, and global efficiency, are also commonly employed. In particular, the FC variability of a specific brain region reflects its dynamic change over time within brain states and is generally estimated by the overall variance of the dFC between networks/regions (Zhang et al., 2016). Differently, flexibility reflects the dynamic reconfiguration of functional connections between

different brain areas that occurs over time and for different tasks (Garcia et al., 2018; Harlalka et al., 2019). Such flexibility could be measured in the context of entropy, which is an index of complexity that characterizes nonlinear properties of resting-state signal (Sokunbi et al., 2011; Wang et al., 2014). Lastly, global efficiency measures the efficiency of information exchange over time in a temporal network (Dai et al., 2016).

In this framework, the overarching goal of this review was to systematically summarize and analyze the extant literature on dFC at resting state in SCZ and BD to identify disease-associated changes.

2. Methods

2.1. Article selection and classification

In February 2022 we conducted a systematic search of the literature on PubMed, Web of Science, and Scopus without any language restriction, in accordance with the Meta-analysis of Observational Studies in Epidemiology guidelines (MOOSE, see Supplementary Materials) (Stroup et al., 2000). A combination of the following keywords was used: “dynamic functional connectivity” OR “dynamic functional network connectivity” OR dFC OR “dynamic network connectivity” OR “dynamic brain network” OR “dynamic brain functional network” OR “dynamic brain connectivity” AND schizophrenia OR “bipolar disorder” OR BD or psychosis. We also included relevant studies appearing in the

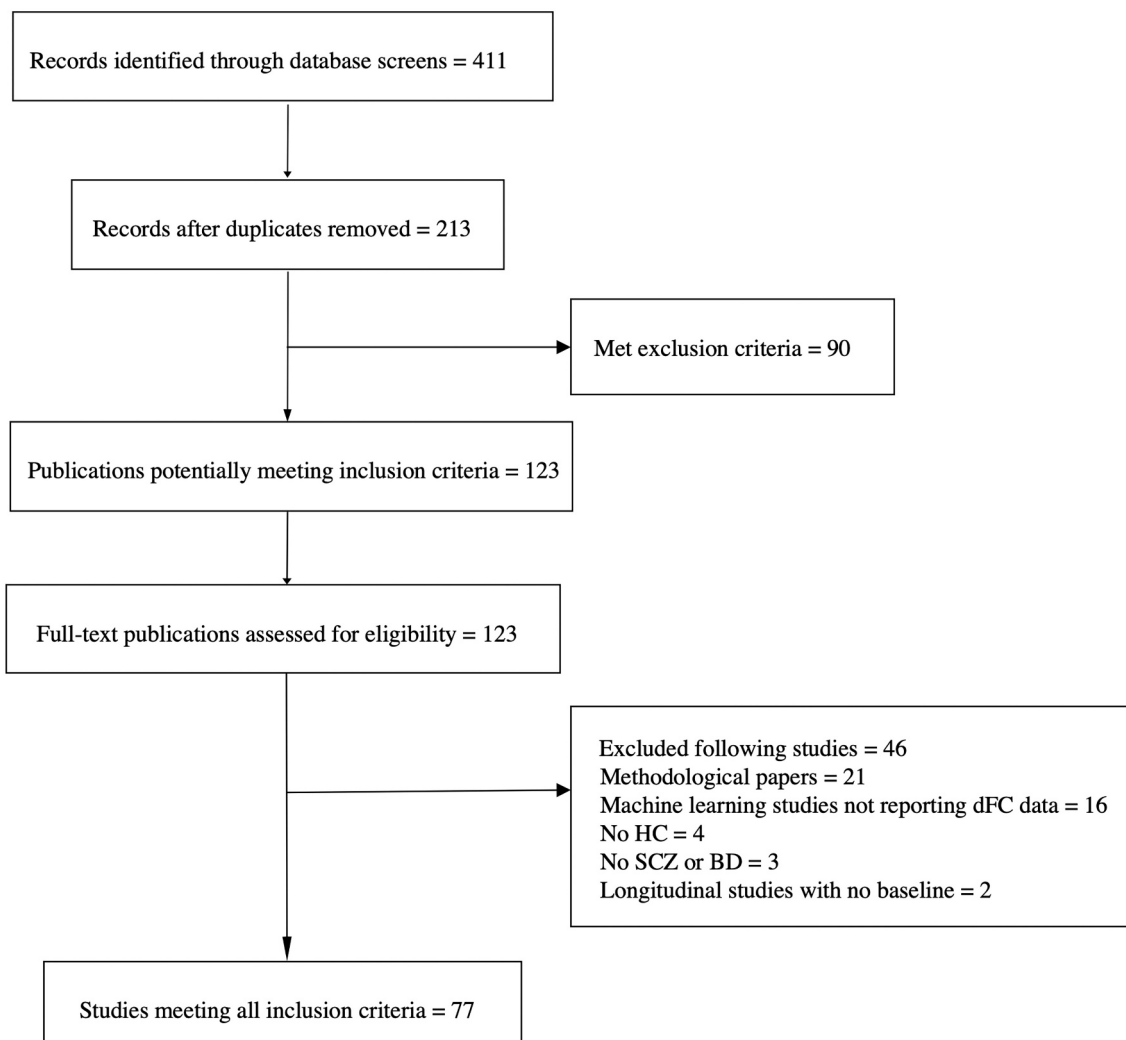


Fig. 1. PRISMA flow chart of the selection of publications for inclusion in the review.

reference lists of the selected articles.

Studies were included if they: 1) estimated dFC; 2) investigated a clinical population affected by BD or/and SCZ; 3) included a healthy control (HC) comparison group. Longitudinal studies were excluded if the baseline dFC was not evaluated.

All selected papers were independently assessed by the authors (GC and FM) and evaluated against inclusion and exclusion criteria. The initial search resulted in 411 articles. The number of duplicates was 198 studies. After reviewing the abstracts of these articles, 123 studies were selected for full-text reading and 43 studies were further excluded because they did not meet the inclusion criteria. Finally, a total of 77 studies were selected (see Fig. 1 for the selection process).

2.2. Data extraction

We used a systematic data extraction procedure to individually determine the main characteristics of the included studies with respect to five categories of variables: 1) population (sample size, age, sex); 2) psychiatric diagnosis; 3) control group (sample size, age, sex); 4) experimental design (methodology, diagnostic tools, dFC pipeline); 5) outcomes (dFC alterations, associations between dFC and psychopathological or cognitive variables).

3. Results

3.1. Studies characteristics

All but four studies (Duan et al., 2020; Lottman et al., 2017; Wang et al., 2021; Zhang et al., 2021) had a cross-sectional design. Overall, 54 studies were carried out in SCZ, 16 in BD, and seven in both disorders. Within SCZ studies, a study was conducted in patients with first-episode psychosis (FEP) (Briend et al., 2020), while two investigations included early-stage SCZ with a duration of the illness of approximately two years (Du et al., 2018; Mennigen et al., 2019). Three investigations explored alterations in dFC in SCZ and in their unaffected relatives (Braun et al., 2016; Guo et al., 2018; Su et al., 2016) and two studies also included individuals at high clinical risk of psychosis (CHR) (Du et al., 2018; Mennigen et al., 2019). Most studies were conducted at rest, and only in 5 studies dFC was calculated during the performance of a task (Braun et al., 2016; Gifford et al., 2020; Li et al., 2020; Sakoğlu et al., 2010; Yue et al., 2018). Eleven studies were conducted on the same sample (Damaraju et al., 2014; Faghiri et al., 2021; Fateh et al., 2020; Fu et al., 2021; Fu et al., 2018; Miller et al., 2016a, 2016b; Rahaman et al., 2021; Salman et al., 2019; Sendi et al., 2021a, 2021b) (see Supplementary Material).

Psychopathological evaluations were carried out using different clinical diagnostic instruments, including the Brief Psychiatric Symptom Scale (BPRS) (Overall and Gorham, 1962), the Hamilton Anxiety Scale (HAM-A) (Hamilton, 1959), the Hamilton Depression Scale (HAM-D) (Hamilton, 1960), the Positive and Negative Affect Scale (PANAS-N) (Watson et al., 1988), the Positive and Negative Symptoms Scale (PANSS) (Kay et al., 1987), the Scale for the Assessment of Negative Symptoms (SANS) (Andersen, 1989), the Scale for the Assessment of Positive Symptoms (SAPS) (Andersen, 1984), the Sign and Symptoms of Psychiatry illness (SSPI) (Liddle et al., 2002), the Structured Interview for Prodromal Syndromes (SIPS) (Miller et al., 2003) and the Young Mania Rating Scale (YMRS) (Young et al., 1978) (see Supplementary Material for a complete list of the clinical scales). Some studies also included functioning and cognitive assessments (see Supplementary Material for details).

The Image acquisition protocols, analytic methods, and clinical assessment tools of the studies are summarized in Tables 1, 2, 3.

3.2. dFC techniques

First, fMRI time series were preprocessed, and then dFC analysis was

performed with the following steps: a) signal extraction to obtain meaningful metrics in terms of raw time series, low-frequency oscillations, regional connectivity, etc.; b) dFC calculation, where several time-dependent connectivity matrices are obtained across the whole time-series; and finally, 3) the estimation of recurring and stable patterns of dFC states at the individual and group level (see Table 4).

3.2.1. Signal extraction

The most widely used technique to obtain time series was spatial group independent component analysis (ICA) (Calhoun et al., 2001). Furthermore, 19 studies explored FC with a seed-based approach that detects the univariate pairwise correlation of one or more a priori-selected seeds or regions of interest (ROI) and other areas of the brain, thus producing seed-based FC maps (Wu et al., 2018). One study investigated the dynamics of regional homogeneity (ReHo) (Dong et al., 2019), which studies the similarity of the time series of a particular voxel with the time series of neighboring voxels, providing a measure of localized FC (Zang et al., 2004). Spontaneous brain activity at rest can be measured not only using the correlation between time series but also by exploring changes in the frequency domain, which is the analysis of the power spectrum that allows the study of specific frequencies of the signal. In particular, the amplitude of low-frequency fluctuations (ALFF) and the fractional amplitude of low-frequency fluctuations (fALFF) detect the intensity of spontaneous low-frequency fluctuations of the BOLD signal in the whole brain (Turner et al., 2013). Here, we included studies that explored the dynamics of ALFF (dALFF) and dynamic fALFF (dfALFF), defined as recurring patterns of ALFF and fALFF variability over time calculated with the sliding window approach and clustered in states (Chen et al., 2022; Fu et al., 2018; He et al., 2021; Liang et al., 2020; Luo et al., 2021; Nyatega et al., 2021). Moreover, Yang et al. (2020) used voxel mirrored homotopic connectivity analysis to investigate the temporal variability of interhemispheric functional connectivity between homotopic areas (Yang et al., 2020) (see Supplementary Material).

3.2.2. dFC calculation

Several techniques were used to study time-varying changes in FC. One of the most widely used was the sliding window (SW) approach, which partitions the time course of the fMRI signal into several fixed temporal windows (that may partially overlap), where pairwise correlations between regions/networks are computed until reaching the end of the time courses itself (Hutchison et al., 2013; Rashid et al., 2014). Then, to assess the frequency and structure of reoccurring FC patterns, a clustering algorithm for windowed covariance matrices is commonly used (Lloyd, 1982) (Fig. 2). In addition, other methods have been used, including: 1) network flexibility, which is a measure of how often a brain area changes its allegiance to a community of nodes over time (Braun et al., 2016); 2) quasi-periodic patterns (QPP), which reflect the spatio-temporal patterns of signal oscillations in the infra-low frequency range and are supposed to underlie functional connectivity (Briend et al., 2020); 3) filter-banked connectivity, an approach that does not make a priori assumptions about connectivity frequency and performs frequency tiling in the connectivity domain (Faghiri et al., 2021); and 4) dynamic directional functional domain connectivity, a method that operates at a dimensional scale sufficient to capture multiplexed dynamical relationships within and between functional domains (Miller et al., 2016b). Four studies explored the effects of global signal regression on dFC findings and three investigations examined frequency-related changes in dFC (see Supplementary Material).

3.2.3. Estimation of connectivity states

k-means clustering is one of the most widely used methods to modularize windowed connectivity patterns. Briefly, *k*-means clustering is an unsupervised technique that automatically partitions a data set into a predefined number (*k*) of clusters, typically spanning from 2 to 20 (Shakil et al., 2014; Supekar et al., 2019). In this context, each state is

Table 1
Selection of studies that evaluate dynamic functional connectivity in schizophrenia.

Author, year	Subjects number (M/F) Age (years) mean \pm SD	Study design	MRI acquisition and dFC analysis	Clinical scales	Duration of illness (years)	Comorbidities	Medications	Neuroimaging findings	Correlations with clinical scales
Bhinge et al., 2019	SCZ: 88 (NR) 37.0 \pm 14.0 HC: 91 (NR) 38.0 \pm 12.0	Cross-sectional	NR SW approach k-means clustering	NR	NR NA	NR NR	NR NR	SCZ vs. HC: reside in or switch to a state that has \uparrow positive correlation within the VIS and between the anterior DMN and frontal component, VIS and parietal component, anterior DMN and frontal component, and cerebellum and VIS component. Reside in or switch to a state that has \uparrow negative correlation between the cerebellum and left EXE.	NR
Braun et al., 2016	SCZ: 28 (17/11) 33.4 \pm 9.2 Rel: 37 (8/29) 29.2 \pm 11.6 HC: 239 (52/87) 32.8 \pm 10.1	Cross-sectional	3 T SW approach (15 TR, 30 s) Working-memory task	SCID-I, PANSS, CGI-S	NR NA NA	NR NR NR	AP stable dose for \geq 2 weeks NR NR	SCZ and Rel vs. HC: \downarrow in network flexibility.	No significant associations between the network flexibility measure in SCZ and PANSS scores.
Briend et al., 2020	FEP: 40 (27/23) 23.4 \pm 5.8 HC: 40 (25/15) 24.8 \pm 6.4	Cross-sectional	3 T SW approach (22 TR, 44 s) k-means clustering (k = 5) ROI (EXE)	BPRS	NR NA	NR NR	AP-naïve NR	FEP vs. HC: \uparrow FCS of the correlation of the QPP in the QPP sliding vector.	No significant associations between BPRS and the FC in the EXE.
Damaraju et al., 2014	SCZ: 151 (114/37) 37.8 \pm NR HC: 163 (117/46) 36.9 \pm NR	Cross-sectional	3 T SW approach k-means clustering (k = 5) (22 TR, 44 s)	NR	NR NA	NR NR	AP NR	SCZ vs. HC: \downarrow time in states typified by strong, large-scale FC.	NR
Deng et al., 2019	SCZ: 40 (25/15) 26 \pm 8.2 HC: 24 (14/10) 26.5 \pm 6.9	Cross-sectional	3 T SW approach k-mean clustering	SCID, PANSS	3.29 \pm 3.59 NA	NR NR	AP NR	SCZ vs. HC: \uparrow mean FC variability of the whole dorsal VIS; \uparrow temporal variability of the right fusiform gyrus in the dorsal network.	Significant positive correlations between the FC variability of the right fusiform gyrus and the PANSS total scores and the PANSS negative scores.
Deng et al., 2021	SCZ positive: 21 (13/8) 26 \pm NR SCZ negative: 19 (12/7) 27 \pm NR HC: 24 (10/14) 27 \pm NR	Cross-sectional	3 T SW approach k-mean clustering	SCID, PANSS	2 \pm NR 2 \pm NR NA	NR NR NR	AP AP NR	SCZ positive vs. HC and SCZ negative: \downarrow mean FC-variability of the whole emotional network and the FC-variabilities in the bilateral anterior insula. SCZ positive: abnormally enhanced negative coupling between variability and FCS.	No significant correlations between any network measurement of interest and the PANSS and PANSS subscale scores in SCZ positive and negative.
Dong et al., 2019	SCZ: 96 (66/30) 39.8 \pm 11.5	Cross-sectional	3 T SW approach (l = 20, 22, 24, ... 40 s)	SCID, PANSS	15.10 \pm 10.3	No comorbid axis I diagnosis	AP 96	SCZ vs. HC: \uparrow variability of regional voxel-level FC in regions widely distributed across VIS, SM, attention, thalamus, and cerebellum	Negative correlation between the positive PANSS subscale scores and the variability of region-to-whole-brain FC in the right lingual gyrus

(continued on next page)

Table 1 (continued)

Author, year	Subjects number (M/F) Age (years) mean \pm SD	Study design	MRI acquisition and dFC analysis	Clinical scales	Duration of illness (years)	Comorbidities	Medications	Neuroimaging findings	Correlations with clinical scales
	HC: 122 (81/41) 38.0 \pm 14.7		clustering Dynamic ReHo		NA	No current or past axis I disorder	NA	SCZ vs. HC: \uparrow variability of FC in brain regions from VIS, SM, attention, and thalamus to the whole brain; \uparrow variability of FC in brain regions from DMN and EXE to the whole brain. SCZ \downarrow within-network variability in VIS, SM, and thalamus; \downarrow within-network variability in DMN and EXE when using two atlases (FDR corrected); \uparrow between-network variability in VIS-thalamus, SM-attentional, SM- thalamus, and \downarrow between-network variability in DMN-EXE.	with Positive correlation between the PANSS negative scores and variability of region-to-whole- brain FC in the right insula. Negative correlation between the PANSS general scores and variability of region-to-whole-brain FC in the nodes of VIS, SM, and thalamus. Negative correlation between PANSS total score and variability of FC in nodes of VIS, SM, and thalamus
Du et al., 2016	SCZ: 82 (65/17) 38.0 \pm 14.0 HC: 82 (63/19) 37.7 \pm 10.8	Cross-sectional	3 T SW approach (20 TR, 40 s) k-mean clustering (k = 2)	SCID, PANSS	NR	NR	NR	SCZ vs. HC: impaired interaction among DMN subsystems, reduced central role for PCC and aMPFC hubs, weaker interaction between dMPFC subsystem and medial temporal lobe subsystem.	NR
Du et al., 2018	SCZ: 58 (38/20) 21.8 \pm 3.8 CHR: 53 (32/21) 20.4 \pm 4.5 HC: 70 (41/29) 21.9 \pm 5.6	Cross-sectional	3 T SW approach (20 TR, 40 s)	SCID, PANSS, SIPS, SOPS	2.08 \pm 1.37 NA	NR	AP 53 AP-naïve 41	SCZ vs. CHR: \uparrow aberrant connectivities and greater alterations in the cerebellum, frontal cortex, thalamus, and temporal cortex. SCZ and CHR vs. HC: common aberrances in the supplementary motor area, parahippocampal gyrus, and postcentral cortex. CHR: specific changes in connections between the superior frontal gyrus and calcarine cortex.	NR
Du et al., 2021b	SCZ: 36 (NR) NR HC: 49 (NR) NR	Cross-sectional	NR time-window approach (20 time points) k-mean clustering (k = 5)	NR	NR NA	NR	NR	SCZ vs. HC: \downarrow FC and \downarrow time in states in which FC between the olfactory region and hippocampus and frontal gyrus and vermis presented the most significant differences, \uparrow FC and \uparrow time in states in which FCs between postcentral gyrus and vermis and thalamus and temporal gyrus showed the most significant differences.	NR
Duan et al., 2020	SCZ: 42 (27/15) 24.9 \pm 4.8 HC: 38 (25/13) 24.8 \pm 4.6	Longitudinal (8-week risperidone)	3 T SW approach (50 TR, 5 TR, 37 windows) ROI: insula	SCID, PANSS	< 1 year	NR	Risperidone 4–6 mg/day for 8 weeks NA	SCZ baseline: \downarrow dFC variance between the insular subdivisions and the precuneus, supplementary motor area, and temporal cortex, \uparrow increased dFC variance between the insular subdivisions and parietal cortex. SCZ after treatment: normalization of dFC variance of the abnormal connections and significant improvement in positive symptoms.	NR
Espinoza et al., 2019	SCZ: 42 (27/15) 24.9 \pm 4.8	Cross-sectional	3 T SW approach (22 TR, 44 s)	NR	NR	NR	NR	SCZ vs. HC: \uparrow time in a state displaying weak connectivity between RSNs from all domains), \downarrow time in states showing stronger within- and between-	NR

(continued on next page)

Table 1 (continued)

Author, year	Subjects number (M/F) Age (years) mean \pm SD	Study design	MRI acquisition and dFC analysis	Clinical scales	Duration of illness (years)	Comorbidities	Medications	Neuroimaging findings	Correlations with clinical scales	
Faghiri et al., 2020	HC: 38 (25/13) 24.8 \pm 4.6	Cross-sectional	k-mean clustering (k = 5)	NR	NA	NR	NR	connectivity in the AUD, VIS, and SM domains compared to the other states.	NR	
	SCZ: 151 (NR) NR HC: 163 (NR) NR		3 T SW approach (window size 3-20) k-mean clustering (k = 3) weighted average of shared trajectory (WAST)		NR	NR	NR	NR		SCZ vs. HC: \uparrow time in a connectivity state with negative connectivity between motor and sensory regions.
Faghiri et al., 2021	SCZ: 151 (NR) NR HC: 163 (NR) NR	Cross-sectional	3 T SW approach (10 TR, 22 s) k-mean clustering (k = 8) filter-banked connectivity	NR	NR	NR	NR	SCZ: weak connection between SM and VIS/AUD networks.	NR	
Fu et al., 2018	SCZ: 151 (114/37) 37.8 \pm 11.4 HC: 163 (117/46) 36.9 \pm 11.0	Cross-sectional	3 T SW approach (20 TR, 40s) k-mean clustering (k = 6) dALFF	NR	NR	NR	Medications	The ALFF of brain regions was highly fluctuating during the resting-state and such dynamic patterns are altered in SCZ. dALFF and dFC were correlated in time, and their correlations are altered in SCZ.	Correlation between dALFF-dFC and cognitive score.	
Fu et al., 2021	SCZ: 151 (115/36) 38.8 \pm 11.6 HC: 160 (115/45) 37.0 \pm 10.9	Cross-sectional	3 T SW approach (20 TR, 40s) Step-wise FNR	SCID, CMINDS	NR	NR	NR	SCZ vs. HC: \uparrow sFNR between SC and SM/VIS/CB domains, between CB and SM/CC/DM domains, and within CB domains.	NR	
Gifford et al., 2020	SCZ: 55 (46/9) 36.1 \pm 13.6 HC: 72 (49/23) 35.9 \pm 11.7	Cross-sectional	3 T SW approach (15 TR, 30 s; 25 TRs, 50 s; 30 TRs, 60 s) k-mean clustering	PANSS	15.0 \pm 12.5	NR	AP	SCZ vs. HC: flexibility scores in cerebellar, subcortical and EXE, in the left thalamus and in the right crus I.	NR	
Guo et al., 2018	SCZ: 28 (15/13) 25.4 \pm 5.8 Rel: 38 (15/13) 25.8 \pm 6.4 HC: 60 (35/25) 27.2 \pm 6.6	Cross-sectional	3 T SW approach (10, 11, ..., 20 volumes, equal to 20, 22, 24, ..., 40 s)	PANSS	1.3 \pm 1.1	NR	NR	AP 21	SCZ vs. HC and Rel: \uparrow instability on the precuneus. Rel vs. SCZ: \uparrow in medial orbitofrontal and \downarrow in putamen instability.	NR
	SCZ: 42 (26/16) 42.1 \pm 10.7 HC: 52 (29/23) 41.5 \pm 12.9		3 T SW approach (50 TR, 100 s)	SCID-I- CV, PANSS	17.3 \pm 9.9	NR	NR	AP 42	SCZ vs. HC: \downarrow dFC between CBCc and CBCm and \downarrow dFC between CBCm and cortical/subcortical networks including EXE, DMN, and SM networks.	NR

(continued on next page)

Table 1 (continued)

Author, year	Subjects number (M/F) Age (years) mean \pm SD	Study design	MRI acquisition and dFC analysis	Clinical scales	Duration of illness (years)	Comorbidities	Medications	Neuroimaging findings	Correlations with clinical scales
He et al., 2021	SCZ: 96 (68/28) 41.7 \pm 11.9 HC: 212 (80/41) 39.9 \pm 14.0	Cross-sectional	3 T SW approach (50 TR, 100 s)	SCID-I-CV, PANSS	15.7 \pm 10.9	NR No psychiatric comorbidities	AP 96 No psychotropic medications	SCZ vs. HC: \downarrow dFC within sensory and perceptual sDFNs, \downarrow dFC between these sDFNs, and high-order frontal sDFNs.	Negative correlation between PANSS-positive scores and dFC within the FCS-sDFN and between the PANSS total score and connectivity between ALFF-sDFNs.
Jia et al., 2017	SCZ: 69 (35/34) 32.0 \pm 9.6 HC: 52 (25/27) 29.9 \pm 8.6	Cross-sectional	3 T SW approach (20 TRs, 40 s) SampEn ROI	DSM-IV, PANSS	7.2 \pm 6.6	NR No psychiatric comorbidities	NR No psychotropic medications	SCZ vs. HC: \downarrow association between SampEn and age.	Association between SampEn between the right amygdala and the right superior orbital frontal gyrus and illness duration and between SampEn between the right amygdala and the left inferior parietal gyrus and PANSS general scores and illness duration.
Jia and Gu, 2019	SCZ: 69 (35/34) 32.0 \pm 9.6 HC: 52 (25/27) 29.9 \pm 8.6	Cross-sectional	3 T SW approach (20 TRs, 40 s) SampEn	DSM-IV, PANSS	7.2 \pm 6.6	NR No psychiatric comorbidities	NR No psychotropic medications	SCZ vs. HC: \uparrow SampEn at the whole-brain level in the VIS and in the AUD network	Positive correlation between PANSS-negative score and SampEn of the right middle occipital gyrus. Positive correlation between PANS positive and general scores and SampEn of the right inferior occipital gyrus. Positive correlation between SampEn of the left superior occipital gyrus and illness duration.
Li et al., 2020 (1)	SCZ: 50 (34/16) 36.5 \pm 8.9 HC: 50 (29/21) 39.1 \pm 6.6	Cross-sectional	3 T SW approach (30 TRs, 60 s) ROI: LOC	NR	NR	NR	AP, AD, MD, anxiolytics	SCZ vs. HC: \uparrow temporal instability of LOC connectivity over time under resting and task-switching conditions. SCZ: during rest \uparrow interaction of LOC with EXE and thalamus; during task \uparrow interaction of LOC with the DMN.	Positive correlation between temporal instability of LOC connectivity and patients' switching cost during task performance and with hallucination severity.
Long et al., 2021	SCZ: 88 (NR) 37 \pm 14 HC: 91 (NR) 38 \pm 12	Cross-sectional	3 T SW approach sliding (24 TRs, 48 s) k-means clustering Graph theory	NR	NR	NR	NR	SCZ vs. HC: dysconnectivity among brain networks. \downarrow centrality in frontal components	NR
Lottman et al., 2017	SCZ: 34 (23/11) 32.4 \pm 10.4 HC: 35 (25/10) 32.0 \pm 8.9	Longitudinal (6-week risperidone)	3 T SW approach (30, 40, 44, 50, 60 s) k-means clustering (k = 3)	DIGS, BPRS	NR	NR	Risperidone 4.36 \pm 1.45 mg at week 6. 12 benzotropine, 4 CE, 1 MS No psychotropic medications	Unmedicated SCZ vs. HC: \uparrow connectivity between the thalamus and somatomotor network, \downarrow time and fraction of time spent in the sparsely connected state, \uparrow time and fraction of time spent in the intermediately connected state. Risperidone normalizes mean dwell times after 6 weeks, but not the fraction of time spent.	NR
Luo et al., 2020	SCZ: 96 (NR) NR HC: 121 (NR) NR	Cross-sectional	3 T SW approach (50 TR, 100 s)	SCID-I-CV, PANSS	NR	NR	AP NR	SCZ vs. HC: \downarrow FCS in SAL, AUD, SM, and VIS networks, \uparrow FCS in the cerebellum, basal ganglia, and EXE networks across different frequency bands.	Partial correlation between FCS of the insula, thalamus, calcarine cortex, orbitofrontal gyrus, and paracentral lobule and clinical symptoms in slow-5 and slow-4 bands.
Mennigen et al., 2019	SCZ: 58 (38/20) 21.8 \pm 3.8	Cross-sectional	3 T SW approach (22 TR, 44 s)	SCID, PANSS, Kiddie-SADS	2.1 \pm 1.4	NR	AP 53	SCZ vs. CHR and HC: \uparrow likelihood of transitioning to a hypoconnected state. HC vs. SCZ and CHR: changes of	NR

(continued on next page)

Table 1 (continued)

Author, year	Subjects number (M/F) Age (years) mean \pm SD	Study design	MRI acquisition and dFC analysis	Clinical scales	Duration of illness (years)	Comorbidities	Medications	Neuroimaging findings	Correlations with clinical scales
	CHR: 53 (32/21) 20.4 \pm 4.5 HC: 70 (41/29) 21.9 \pm 5.6		k-means clustering (k = 5)		NA	NR	AP 12	connectivity between states that were absent or altered in SCZ and CHR.	
Miller et al., 2016a	SCZ: 151 (NR) 37.8 \pm NR HC: 163 (NR) 36.9 \pm NR	Cross-sectional	3 T SW approach (22 TRs, 44 s) k-means clustering (k = 5)	NR	NR	NR	NR	SCZ vs. HC: less dynamically active time-varying whole-brain network connectivity patterns, especially in patients with high levels of hallucinatory behavior.	NR
Miller et al., 2016b	SCZ: 151 (NR) 37.8 \pm NR HC: 163 (NR) 36.9 \pm NR	Cross-sectional	3 T SW approach (22 TRs, 44 s) k-means clustering (k = 15) ddFDC	NR	NR	NR	NR	SCZ vs. HC: \downarrow FCS and dynamism.	NR
Okanda Nyatega et al., 2021	SCZ: 72 (14/58) 38.17 \pm 13.89 HC: 74 (23/51) 35.82 \pm 11.58	Cross-sectional	3 T SW approach (15 TRs, 30 s)	SCID	16 \pm 12.4	SAFF, BD	NR	SCZ vs. HC: \downarrow mean FCS between cuneus and calcarine, cuneus and lingual gyrus, cuneus, and middle temporal gyrus.	NR
Plis et al., 2018	SCZ: 144 (110/34) 38.0 \pm NR HC: 154 (110/44) 37.0 \pm NR	Cross-sectional	3 T SW approach k-means clustering (k = 5)	NR	NR	NR	NR	SCZ vs. HC: \uparrow time in states where most ICs exhibit weaker FC. HC vs. HC: \uparrow transitions in states that present high to moderate correlations among many IC.	NR
Rabany et al., 2019	SCZ: 33 (25/8) 24.8 \pm 0.5 HC: 34 (23/11) 23.7 \pm 0.6	Cross-sectional	3 T SW approach (33 s, step = 1TR) k-means clustering (k = 4)	PANSS	NR	NR	NR	Number of different states: \downarrow in SCZ SCZ vs. HC: \downarrow number of transitions, \uparrow fraction of time in a state of weak, intra-network connectivity, \downarrow fraction of time in a highly connected state, \downarrow fraction of time in a widely connected state, \uparrow time in the weakly-connected state, and \downarrow in the highly-connected state.	No significant associations between PANSS and PANSS subscales.
Rahaman et al., 2021	SCZ: 151 (114/37) 37.8 \pm NR HC: 163 (117/46) 36.9 \pm NR	Cross-sectional	3 T SW plus clustering (22 TR, 44 s) Statelets	NR	NR	NR	NR	SCZ group statelets can characterize fewer pairs since the links are more disrupted. HC connections are more synchronized at each time point.	NR
Sakoğlu et al., 2010	SCZ: 28 (23/5) 36.4 \pm 12.4 HC: 28 (19/9) 28.8 \pm 10.7	Cross-sectional	3 T SW approach (96 s)	DSM-IV TR	NR	NR	NR	SCZ vs. HC: \uparrow task-modulation of motor-frontal, lateral fronto-parietal –medial temporal, and posterior DMN-parietal connections. HC vs. SCZ: \uparrow task modulation of orbitofrontal-DMN and medial temporal-frontal connections.	NR

(continued on next page)

Table 1 (continued)

Author, year	Subjects number (M/F) Age (years) mean \pm SD	Study design	MRI acquisition and dFC analysis	Clinical scales	Duration of illness (years)	Comorbidities	Medications	Neuroimaging findings	Correlations with clinical scales
Salman et al., 2017	SCZ: 186 (NR) HC: 176 (NR) NR	Cross-sectional	3 T SW approach (22 TR, 44 s) k-means clustering (k = 3)	DSM-IV TR, SAPS, SANS, PANSS	NR NA	NR NR	NR NR	SCZ vs. HC: have \uparrow state probabilities in the SM-DMN dFC and state probabilities in VIS- DMN dFC. \uparrow entropy in the SC-SC, FRN-VIS, and DMN-VIS dFC. \downarrow CDMI in SC-SM vs. SC-VIS, SM-ATTN vs. VIS-ATTN and SM-ATTN vs. ATTN-ATTN dFC pairs. SCZ vs. HC: \uparrow dFC in SC and SM networks; \downarrow FCS between AUD, VIS, and SM networks; abnormal connectivity in DMN.	Positive correlation between PANSS positive scores and the VIS-FRN vs VIS-DMN CDMI.
Salman et al., 2019	SCZ: 82 (65/17) 38.0 \pm 14.0 HC: 82 (63/19) 37.7 \pm 10.8	Cross-sectional	3 T SW approach (26 TR and step of 1 TR) k-mean clustering (k = 5) Affinity propagation clustering	NR	NR NA	NR NR	NR NR	SCZ vs. HC: \uparrow transformed entropy in SCZ in the following pairs: SC-SC, DMN-SC, CB-AUD, and CB-ATTN. \downarrow CDMI in the following pairs: SC-VIS and SC-AUD, AUD-AUD and SC-AUD, AUD-SM and AUD-AUD, SM-ATTN and AUD-ATTN, SM-FRN and AUD- FRN, VIS-ATTN, and SM-ATTN as well as VIS-FRN and SM- FRN.	NR
Salman et al., 2019	SCZ: 151 (114/37) 37.8 \pm NR HC: 163 (117/46) 36.9 \pm NR	Cross-sectional	3 T SW approach (22 TR, 44 s) k-means clustering (k = 3)	NR	NR NA	NR NR	NR NR	SCZ vs. HC: \downarrow time in a state typified by strong, large-scale FC.	NR
Sanfratello et al., 2019	SCZ: 46 (NR) NR HC: 45 (NR) NR	Cross-sectional	3 T SW approach (22 TR, 44 s) k-mean clustering (k = 4)	SCID-IV	NR NA	NR NR	NA NR	SCZ vs. HC: \downarrow dFC of ACC, \uparrow dFC between the precuneus and the PCC.	NR
Sendi et al., 2021a	SCZ: 68 (57/11) 37.8 \pm 14.4 HC: 89 (64/25) 38.1 \pm 11.7 SCZ: 151 (115/36) 38.1 \pm 11.3 HC: 160 (115/45) 37.0 \pm 10.7	Cross-sectional	3 T SW approach (20 TR, 40 s) k-mean clustering (k = 5)	SCID-IV, SCID-I/NP interview, PANSS	< 1 NA	NR No psychiatric comorbidities	stable dose of AP for at least 2 months No psychotropic medications	SCZ vs. HC: \downarrow dFC of ACC, \uparrow dFC between the precuneus and the PCC.	Transition probability from a state with weaker precuneus/PCC and stronger ACC dFC to a state with stronger precuneus/PCC and weaker ACC dFC increased with symptom severity.
Sendi et al., 2021b	SCZ: 151 (115/36) 38.1 \pm 11.3 HC: 160 (115/45) 37.0 \pm 10.7	Cross-sectional	3 T SW approach (20 TR, 40 s) k-mean clustering (k = 5) ROI: visual sensory network	SCID-IV, SCID-I/NP interview, PANSS	< 1 NA	NR No psychiatric comorbidities	stable dose of AP for at least 2 months No psychotropic medications	HC vs. SCZ: \uparrow dFC in cuneus and middle temporal gyrus connectivity in all states. States 2, 3: \downarrow differences between HC and SCZ in the dFC of calcarine gyrus with other regions of VS-N. State 4: \downarrow differences between calcarine gyrus and other regions. State 5: the greatest difference between HC and SCZ in the dFC of the middle temporal gyrus and other regions within the VS.N + significant difference in connectivity of lingual and fusiform gyri.	Positive correlation between visual learning memory and state 4 occupancy rate in SCZ.

(continued on next page)

Table 1 (continued)

Author, year	Subjects number (M/F) Age (years) mean \pm SD	Study design	MRI acquisition and dFC analysis	Clinical scales	Duration of illness (years)	Comorbidities	Medications	Neuroimaging findings	Correlations with clinical scales				
Sheng et al., 2021	SCZ: 51 (40/11) 38.1 \pm 13.8	Cross-sectional	3 T SW approach	SCID DSM-IV	NR	NR	NR	SCZ vs. HC: \downarrow FCS and \uparrow variability FC widespread across the brain dynamic subnetworks.	NR				
	HC: 63 (42/21) 36.3 \pm 12.1									NA	NR	NR	
	SCZ: 36 (28/8) 37.2 \pm 9.3									NR	NR	NR	
	HC: 60 (36/24) 33.7 \pm 9.0									NA	NR	NR	
Su et al., 2016	SCZ: 25 (NR) NR	Cross-sectional	3 T SW approach (20 TRs, 40 s) k-mean clustering (k = 8)	SCID DSM-IV, PANSS	NR	NR	AP 19	SCZ and Rel vs. HC: altered dFC between aPFC- right precuneus, between the leftFG- leftITG, between the left anterior insula - left ITG, between left anterior insula- the right AG, and between left ventromedial PFC - right medial occipital lobe.	NR				
	Rel: 25 (NR) NR									NA	No psychiatric comorbidities	No psychotropic medications	
	HC: 25 (NR) NR									NA	No psychiatric comorbidities	No psychotropic medications	
Sun et al., 2019	SCZ: 18 (10/8) 38.8 \pm 9.9	Cross-sectional	3 T SW approach (50 TRs, 100 s) temporal efficiency approach and temporal random network model	SCID-IV, PANSS, GAF	11.6 \pm 8.4	NR	AP	SCZ: localized changes of temporal nodal properties in the left frontal, right medial parietal, and subcortical areas	Positive correlation between the temporal regional efficiency in the left orbitofrontal and PANSS positive scores.				
	HC: 19 (10/9) 37.7 \pm 9.0									NA	No psychiatric comorbidities	No psychotropic medications	
	SCZ: 53 (41/12) 38.3 \pm 13.9									15.6 \pm 12.0	NR	AP	Negative correlation between the temporal regional efficiency in the precuneus and left temporal pole and PANSS negative scores.
	HC: 57 (37/20) 35.4 \pm 11.9									NA	No psychiatric comorbidities	No psychotropic medications	Positive correlation between the temporal regional efficiency in the left orbitofrontal and PANSS general scores.
Sun et al., 2021	SCZ: 28 (15/13) 16.8 \pm 1.2	Cross-sectional	3 T SW approach (50 TRs, 100 s) k-mean clustering (k = 6) ROI: mirror neuron system, mentalizing network	Structured Clinical Interview for DSM-IV TR, PANSS	0.7 \pm 0.8	NR	AP-naïve	SCZ vs. HC: \downarrow FCS between the right temporo-parietal junction and right inferior frontal gyrus and between the left inferior parietal lobe and left middle temporal gyrus; between the right temporo-parietal junction and right inferior frontal gyrus; between the right temporo-parietal junction and right inferior frontal gyrus and between right inferior frontal gyrus and left the extrastriate visual area; between the right temporo-parietal junction and right inferior frontal gyrus and between left middle temporal gyrus and left the extrastriate visual area; between the right temporo-parietal junction and right inferior frontal gyrus between left middle	Negative correlation between dFC between the left middle temporal gyrus and lthe eft extrastriate visual area and item 2 of PANSS negative score.				
	HC: 22 (10/12) 16.3 \pm 2.3									NA	NR	NR	

(continued on next page)

Table 1 (continued)

Author, year	Subjects number (M/F) Age (years) mean \pm SD	Study design	MRI acquisition and dFC analysis	Clinical scales	Duration of illness (years)	Comorbidities	Medications	Neuroimaging findings	Correlations with clinical scales
Supekar et al., 2019	SCZ: 35 (30/5) 34.4 \pm 12.6 HC: 35 (24/11) 36.0 \pm 12.2 SCZ: 30 (21/9) 31.5 \pm 10.4 HC: 30 (14/16) 33.8 \pm 13.1	Cross-sectional	3 T SW approach (50 TRs, 100 s) k-mean clustering (k = 2-20)	SCID, PANSS	NR NA NR NA	NR NR	AP, AD, MS, anxiolytics NA AP, AD, MS, anxiolytics NA	temporal gyrus and right extrastriate visual area. SCZ vs. HC: In both cohorts, dynamic SAL-centered cross-network interactions were significantly reduced, less persistent, and more variable in SCZ.	Correlations between dynamic time-varying measures of SN-centered cross-network interactions and PANSS positive scores in both cohorts.
Wang et al., 2016	SCZ: 30 (21/9) 31.5 \pm 10.4 HC: 30 (14/16) 33.8 \pm 13.1	Cross-sectional	3 T flexible least squares (FLS) method	SCID, PANSS	14.6 \pm 1.6 NA	NR No psychiatric comorbidities	AP No psychotropic medications	SCZ vs. HC: \uparrow variances of the inter-network FC between the DMN and the EXE and between the DMN and the SAL and within the SAL.	NR
Wang et al., 2019b	EOS: 35 (20/15) 15.5 \pm 1.8 HC: 30 (13/17) 15.3 \pm 1.6	Cross-sectional	3 T SW approach (50 TRs, 100 s; widow width = 30TRs/40TRs, step = 10TRs and widow width = 50TRs, step = 2TRs/5TRs) k-mean clustering (k = 5)	SCID-IV-TR, PANSS	1.3 \pm 1.2 NA	No comorbid Axis I diagnosis No psychiatric comorbidities	drug-naive No psychotropic medications	EPS vs. HC: \downarrow dFC in the right middle temporal gyrus, left middle temporal gyrus, left precuneus, and left calcarine. \uparrow dFC in the left cerebellum crus, left middle cingulate gyrus, right putamen, right precuneus, and right supramarginal gyrus.	Negative correlations between the left cerebellum crus1 with \downarrow FC and PANSS negative scores. Negative correlations between the right supramarginal gyrus with \downarrow FC and the PANSS general and total scores. Negative correlations between the right putamen with \downarrow FC and the PANSS total scores.
Wang et al., 2021	SCZ: 64 (31/33) 24.7 \pm 6.8 HC: 67 (32/35) 24.2 \pm 6.1	Longitudinal (12-week AP treatment)	3 T SW approach k-mean clustering ROI: triple network	SCID-IV, PANSS, MINI	NR NA	NR No psychiatric comorbidities	Baseline: drug-naive AP 64 No psychotropic medications	HC vs. SCZ at baseline: mean lifetime of state 1 and state 2 \downarrow . After medication, the mean lifetime of corresponding brain states was significantly extended. At baseline, the mean value of dNIIs across dynamic brain states was \downarrow .	Significant quadratic relationship between the longitudinal change in mean dNII and the reduction ratio in PANSS total score after treatment.
Weber et al., 2020	SCZ: 80 (59/21) 31.0 \pm 11.9 HC: 80 (NR) 30.9 \pm 11.1	Cross-sectional	3 T SW approach (20 TRs, 40 s) k-mean clustering (k = 5)	ICD-1, PANSS	4.8 \pm 7.7 NA	NR NR	AP, 8 CE, MS 6, opioids 1, anxiolytics 13, anticholinergic 4, PS 1 NR	SCZ vs. HC: \uparrow dwell time in a state characterized by mostly positive FC which was strong within networks, in particular, the DMN and LAN network, and \downarrow time in a state characterized by strong positive FC within and between sensory networks and by negative FC between sensory and SC networks.	Association between hallucination proneness over 1-year and reduced dwell times in State 1.
Yang et al., 2022	SCZ: 38 (15/23) 36.1 \pm 6.2 HC: 31 (12/19) 32.2 \pm 5.8	Cross-sectional	3 T SW approach (30 TR, 22.5 s) k-mean clustering (k = 5)	SCID-IV, PANSS,	11.3 \pm 6.8 NA	NR NR	Medications NR	SCZ vs. HC: \downarrow time in the sparsely connected state. \downarrow FCS between the VIS and EXE.	Positive correlation between fraction time in state 3 and PANSS negative scores.

(continued on next page)

Table 1 (continued)

Author, year	Subjects number (M/F) Age (years) mean \pm SD	Study design	MRI acquisition and dFC analysis	Clinical scales	Duration of illness (years)	Comorbidities	Medications	Neuroimaging findings	Correlations with clinical scales
Yue et al., 2018	SCZ: 33 (11/22) 30.6 \pm 8.1 HC: 34 (14/20) 28.1 \pm 6.5	Cross-sectional	3 T SW approach (36 s)	SCID, PANSS	4.74 \pm 2.5 NA	NR NR	AP 26 NR	SCZ vs. HC: \uparrow temporal variability of FC between the left amygdala and medial prefrontal cortex.	Negative correlation between the variability of connectivity and cognitive performance on the digit symbol coding task. Marginal positive correlation between the variability of connectivity and symptom severity.
Zarghami et al., 2020	SCZ: 51 (43/8) 35.9 \pm 13.4 HC: 68 (18/50) 35.4 \pm 11.8	Cross-sectional	3 T SW approach k-mean clustering (k = 8)	SCID-I	NR NA	NR NR	NR NR	SCZ vs. HC: \downarrow time in a globally coherent state, subcortical-centered state, and \uparrow time in states reflecting anti coupling within the EXE network. Metastate occupation balance altered in SCZ. The trajectory of IPS patterns is less efficient, less smooth, and more restricted in SCZ.	NR
Zhang et al., 2016	SCZ AH+: 18 (9/9) 35.2 \pm 13.0 SCZ AH-: 17 (12/5) 30.0 \pm 10.1 HC: 22 (9/13) 34.9 \pm 13.3	Cross-sectional	3 T SW approach (100 TRs, 42.7 s) k-mean clustering (k = 5) ROI: eloquent language cortex in the left hemisphere	SCID-I, PANSS	5.9 \pm 6.9 4.0 \pm 3.5 NA	NR NR NR	AP 18 AP 17 NR	No significant findings were observed in any connectivity measures between ROIs at any frequency band.	No significant correlations.
Zhang et al., 2021	SCZ: 34 (17/17) 27.1 \pm 6.1 HC: 28 (13/15) 27.1 \pm 4.5	Longitudinal (8-week AP)	3 T SW approach (22 TR, 44 s) k-mean clustering (k = 5)	SCID-I, MINI, PANSS	0.5 \pm 1 NA	NR No psychiatric comorbidities	Baseline: drug-naïve AP 24 No psychotropic medications	SCZ vs. HC: significant difference in FC variance between both groups at baseline. \downarrow FC variability within DMN and EXE, as well as between multiple other RSNs (i.e., DMM and AUD, SM, CC, CB; CC and AUD, CB; SM and VIS, CB). FC variability \uparrow after treatment in SCZ.	Negative correlation between FC variability correlated with and PANSS total score after treatment.

ACC: anterior cingulate cortex, AG: angular gyrus, AH: auditory hallucinations, aMPFC: anterior medial prefrontal cortex, AP: antipsychotic, aPFC: anterior prefrontal cortex, ATTN: attention, AUD: auditory, BPRS: Brief Psychiatric Rating Scale, BRSNS: between resting state network synchronization, CB: cerebellar, CBCc: Cerebellar cognitive cluster, CBCm: cerebellar motor cluster, CC: cognitive control, CDMI: Cross-Domain Mutual Information, CGI-S: Clinical Global Impression Scale, CHR: clinical high-risk, CMINDS: Computerized Multiphasic Interactive Neurocognitive System, dALFF: dynamic amplitude of low-frequency fluctuation, ddFDC: dynamic directional functional domain connectivity, dFC: dynamic functional connectivity, dFDC: dynamic functional domain connectivity, DIGS: Diagnostic Interview for Genetic Studies, DLPFC: dorsolateral prefrontal cortex, dMPFC: dorsal medial prefrontal cortex, DMN: default mode network, dNII: dynamic network interaction index, EOS: early-onset schizophrenia, EXE: executive network, FC: functional connectivity, FCS: functional connectivity strength, FEP: first-episode psychosis, FG: fusiform gyrus, FNR: functional network reconfiguration, FPN: frontoparietal network, FRN: frontal, GAF: global assessment of functioning, IPS: instantaneous phase synchrony, ITG: inferior temporal gyrus, LOC: lateral occipital cortex, MINI: Mini International Neuropsychiatric, mVN: medial visual network, MTL: medial temporal lobe, PANSS: Positive and Negative Syndrome Scale, PCC: posterior cingulate cortex, PCUN: precuneus, QPP: quasiperiodic patterns, rECN: right executive-control network, Rel: unaffected first-grade relatives, ROI: region of interest, RSNS: resting-state networks, SAPS: Scales for the Assessment of Positive Symptoms, SANS: Scales for the Assessment of Negative Symptoms, SADS: Schedule for Affective Disorders and Schizophrenia for School-Age Children, SampEn: sample entropy, SC: subcortical, SCID-IV: Structured Clinical Interview for DSM IV, sDFN: spatial organization of dynamic functional network, SIPS: Structured Interview for Prodromal Syndromes, SM: sensorimotor network, SMA: supplementary motor area, SOPS: Scale of Prodromal Symptoms, SW: sliding window, SWPC: sliding window Pearson correlation, VIS: visual.

mutually exclusive and the time spent in a specific connectivity state is defined as dwell time. Also, the dFC was measured using spatio-temporal meta-state analysis. Recently, cross-domain mutual information (CDMI) that uses mutual information (i.e., mutual dependence between pairs of variables adopted from a measure from information theory) within the brain networks belonging to the same functional domain has been used to estimate dFC thus including linear and nonlinear relationships (Salman et al., 2017). See the Supplementary Material for other dFC techniques.

In the following paragraphs, for each network we will use this approach: first, we will describe the magnitude of the dFC (FCS), then its variability, and its interaction with other networks. Changes in dFC in SCZ and BD in terms of FCS and variability are illustrated in Fig. 3.

3.3. dFC alterations in SCZ vs. healthy subjects

3.3.1. Global connectivity

A general pattern of dynamic dysconnectivity between brain networks was reported in SCZ (Long et al., 2021). Consistent with this, both increases and decreases in dFC were described in different frequency bands, mainly distributed in the triple network, cerebellum, VIS, SM, and the subcortical network (Luo et al., 2020). Importantly, several studies showed that SCZ spent less time in globally coherent and subcortical-centered states (Damaraju et al., 2014; Espinoza et al., 2019; Sanfratello et al., 2019; Zarghami et al., 2020) and in states with high within- and between-FC of sensory networks (Weber et al., 2020), while they dwelled longer in states characterized by strong FC within networks (in particular, the DMN and the language network) (Weber et al., 2020). Differently, Plis et al. (2018) showed that SCZ made significantly more transitions to states characterized by weaker connectivity within most brain networks (subcortical, AUD, VIS, SM, EXE, DMN, and cerebellum) (Plis et al., 2018). A reduction in time-varying connectivity patterns in the whole-brain networks was reported (Miller et al., 2016c; Rabany et al., 2019), particularly in patients with more severe hallucinations (Miller et al., 2016b). Moreover, SCZ presented increased entropy and reduced cross-domain mutual information, which is a measure of dependence across sets of related brain areas grouped for anatomical and functional associations, indicating reduced dynamic changes in brain connectivity (Salman et al., 2019; Salman et al., 2017). Stepwise functional network reconfiguration (sFNR), a measure reflecting the global ability to rewire brain networks, was increased in large-scale brain networks, including SM, VIS, EXE, and DMN, thus reflecting an increased temporal variability of the networks and, therefore, their instability (Fu et al., 2021). Finally, when selectively investigating the low-frequency bands, SCZ had more occurrences of states characterized by weaker widespread dALFF patterns and fewer occurrences of strong dALFF states in most brain networks, particularly the AUD, SM, VIS, and subcortical networks (Fu et al., 2018).

3.3.2. Default mode network

Within-DMN dFC was reduced (Du et al., 2016; Luo et al., 2020; Salman et al., 2019; Sendi et al., 2021a), although posterior DMN (i.e., right medial parietal cortex) showed increased temporal global efficiency (Sun et al., 2019). The variability of DMN was reduced (Dong et al., 2019). Furthermore, synchronizability, modularity, recurrence, and consistency of the statelets in the DMN were decreased, suggesting that SCZ exhibit more erratic and less efficient communication between the DMN and other brain networks (Rahaman et al., 2021) (see Supplementary Material for the definition of statelets). Between-network dFC revealed that SCZ dwelled in or switch to a state with high positive connectivity between DMN and EXE (Bhinge et al., 2019).

3.3.3. Executive and attention network

Patients presented either a general reduction (Long et al., 2021) or an increase (Luo et al., 2020) in within-EXE functional FCS, and spent more time in states with weaker FCS in this network (Zarghami et al., 2020).

The contribution of QPP to FCS was greater in EXE in FEP (Briend et al., 2020), suggesting a greater impact of QPP on intrinsic brain activity in these subjects. In contrast, the frontal cortex had a lower state-specific FCS in all the states (Sun et al., 2021) and higher temporal nodal efficiency, which assesses the efficiency of information transfer between nodes in a temporal network (Sun et al., 2019). Additionally, patients with SCZ demonstrated a decrease in state-specific FCS between EXE and the cerebellar motor cluster (He et al., 2019) and between EXE and VIS (Yang et al., 2022). Regarding variability measures, higher flexibility scores were reported in SCZ in the EXE (Gifford et al., 2020), along with increased voxel-wise, region-wise, and network-wise FC variability in the attention network (Dong et al., 2019).

3.3.4. Salience network

SAL FCS and within-network connectivity were reduced in different frequency bands in SCZ (Luo et al., 2020). Between-network dynamic interactions of SAL-centered cross-networks within the triple-network model were significantly reduced, less persistent, and more variable in patients (Supekar et al., 2019; Wang et al., 2016).

3.3.5. Sensory-motor network

FCS was increased in the motor network (Du et al., 2021a), but showed high variability and reduced interaction with other networks. In particular, flexibility and variability were higher in the cerebellar, subcortical, and thalamic areas in SCZ (Gifford et al., 2020). Conversely, FCS between the motor and the EXE, DMN, and SM (He et al., 2019), as well as between the SM and the VIS and AUD (Faghiri et al., 2021), was reduced. Additionally, SCZ dwelled less in states with the predominance of sensory and motor networks (Faghiri et al., 2020; Sendi et al., 2021a). Lastly, the synchronizability, modularity, recurrence, and consistency of the statelets were reduced (Rahaman et al., 2021).

3.3.6. Visual networks

FCS was reduced in VIS (Sheng et al., 2021) and also between VIS and the EXE (Yang et al., 2022), AUD and SM networks (Salman et al., 2017), and the mirror system network (Sun et al., 2021). A higher sample entropy was observed in the right middle occipital gyrus (Jia and Gu, 2019), while the lateral occipital cortex showed an increased interaction with EXE and the thalamus at rest, and with DMN during task switching (Li et al., 2020). Synchronizability, modularity, recurrence, and consistency in VIS networks were reduced (Rahaman et al., 2021) and FC variability was increased in dorsal VIS (Deng et al., 2019).

3.3.7. Emotional network

The FC variability was reduced within the emotional network (Deng et al., 2021), and increased between the amygdala-prefrontal network in SCZ (Yue et al., 2018).

3.3.8. Subcortical and other networks

Higher flexibility scores (Gifford et al., 2020) and temporal global efficiency (Sun et al., 2019) were reported in subcortical areas. Decreased FCS was also reported between the olfactory cortex and the hippocampus, and this may be part of altered sensory integration patterns in this disorder (Du et al., 2021a).

3.3.9. dFC alterations in relatives of SCZ and CHR

Mixed results in small samples have been reported in unaffected siblings of SCZ. A small study found dysconnectivity within DMN, SAL and VIS (Su et al., 2016), with a general and nondomain-specific increase in network flexibility (Braun et al., 2016). Other studies investigating whole-brain FC in relatives (Guo et al., 2018) and general dFC (Du et al., 2018), and transitions (Mennigen et al., 2019) between states in clinical high-at-risk individuals (CHR) did not find differences between individuals at risk and HC.

Table 2
Selection of studies that evaluate dynamic functional connectivity in bipolar disorder.

Author, year	Subjects number (M/F) Age (years) mean \pm SD	Study design	MRI acquisition and DFNC analysis	Clinical scales	Current clinical status	Duration of illness	Comorbidities	Medications	Neuroimaging findings	Correlations with clinical scales
Chen et al., 2022	BD II: 128 (63/65) 26.28 \pm 9.15 MDD:143 (56/84) 27.68 \pm 11.52 HC: 132 (61/71) 29.09 \pm 8.80	Cross-sectional	3 T SW approach TDA ROI: striatum	HAMD, YMRS	Depression Depression NA	44.2 \pm 58.79 months 31.19 \pm 39.86 months NA	No comorbidities NR	Drug-naïve or free NR	BD II and MDD vs. HC: \uparrow dFC variability between left putamen and left supplementary motor area and between right putamen and right inferior parietal lobule. BD II vs. MDD and HC: \uparrow dFC variability between right putamen and left precentral gyrus.	No significant correlations between different dFC variability of striatum seeds and any clinical variable.
Du et al., 2021b	BD I: 35 (13/22) 31.49 \pm 8.17 HC: 30 (15/15) 28.87 \pm 7.25	Cross-sectional	3 T SW approach k-means clustering	DSM IV, YMRS, HAMD	Euthymia NA	8.51 \pm 6.46 years NA	No comorbidities NR	MS 35 NR	BD vs. HC: \uparrow frequent transitions between states close to high-level cognitive networks and low-level sensory networks.	NR
Fateh et al., 2020	BD: 40 (22/18) 34.43 \pm 10.76 MDD: 61 (28/33) 34.55 \pm 10.97 HC: 63 (33/30) 31.76 \pm 10.58	Cross-sectional	3 T SW approach ROI: amygdala	DSM IV, HAMD	Depression Depression NA	98.30 \pm 92.16 months 58.59 \pm 62.88 months NA	No comorbidities NR	AD, MS, AP AD monotherapy NR	BD vs. HC: \downarrow dFC between right lateral basal amygdala and left postcentral gyrus; \uparrow dFC between right centromedial amygdala and right cerebellum.	NR
Han et al., 2020	BD: 40 (18/22) 34.43 \pm 10.76 MDD: 61 (33/28) 34.56 \pm 11.07 HC: 63 (33/30) 31.76 \pm 10.50	Cross-sectional	3 T SW approach (50 TRs 100 s and 25 TRs, 50 s)	DSM-IV-TR, HAMD	Depression, euthymia, mania with psychotic symptoms Depression NA	NR NA	No comorbidities NR	Medication 92.50% Medication 98.36% NR	BD vs. MDD vs. HC: different network switching rate of regions in DMN, SAL, and the left striatum. BD and MDD vs. HC: \downarrow network switching rate in the key hubs of DMN.	NR
Liang et al., 2020	BD I: 18 (10/8) 31.67 \pm NR HC: 19 (12/7) 32.16 \pm 10.35	Cross-sectional	1.5 T dALFF	DSM-IV, BRMS, VFT	Depression, euthymia, mania with Psychotic symptoms NA	NR NA	No comorbidities NR	AP, MS NR	BD I vs. HC: \downarrow dALFF in the posterior cingulate cortex, between the posterior cingulate cortex and middle prefrontal cortex.	Positive correlation between the posterior cingulate cortex - middle prefrontal cortex dFC and the VFT in BD I.
Liu et al., 2021	BD: 20 (10/10) 35.17 \pm 9.94 BD: 23 (13/10) 39.17 \pm 13.10 HC: 31(16/15) 33.00 \pm 8.92	Cross-sectional	3 T SW approach (window length = 50 TRs, step length = 20 TRs)	HAMD, YMRS	First depressive episode Euthymia NA	NR NA	No NR	Drug-naïve Lamotrigine NR	BD depressed vs. BD euthymic: \uparrow between SM and DMN and within DMN. BD euthymic vs. HC: abnormalities fronto-striato-thalamic circuit.	NR
Luo et al., 2021	BD: 106 (63/65) 26.08 \pm 8.66 MDD: 114 (56/84) 27.81 \pm 9.72	Cross-sectional	3 T SW approach dALFF Seed: bilateral precuneus + PCC	HAMD, YMRS	Depression NA	46.02 months \pm NR 29.39 \pm NR	No comorbidities NR	Drug-naïve or free Drug-naïve or free	BD and MDD vs. HC: \downarrow temporal variability of the dALFF in the bilateral posterior cingulate cortex/precuneus; \downarrow dFC between the bilateral posterior cingulate cortex/precuneus and the left inferior parietal lobule.	NR

(continued on next page)

Table 2 (continued)

Author, year	Subjects number (M/F) Age (years) mean \pm SD	Study design	MRI acquisition and DFNC analysis	Clinical scales	Current clinical status	Duration of illness	Comorbidities	Medications	Neuroimaging findings	Correlations with clinical scales
Nguyen et al., 2017	HC: 130 (61/71) 28.64 \pm 8.4	Cross-sectional	3 T ROI: DMN	HAMD, YMRS, PANSS, D-KEFS, Trail Making, CWI	NA	NA	NR	NR	BD vs. HC: altered dFC between the middle prefrontal cortex and posterior cingulate cortex, \downarrow variability in the DMN.	Association between \downarrow connectivity variability and slower processing speed and \downarrow cognitive set-shifting in BD.
	BD: 21 (7/14) 47.2 \pm 11.8				euthymia	NR	No comorbidities	48 CE%, AP 52%, MS 67%, anxiolytics 43%		
Pang et al., 2018	HC: 20 (6/14) 47.3 \pm 13.1	Cross-sectional	3 T SW approach (50 TR, 100 s) ROI: the right anterior insula	HAMD	NA	NR	NR	NR	BD and MDD vs. HC: \downarrow dFC between right anterior insula and right ventrolateral prefrontal cortex.	NR
	BD: 30 (14/16) 35.13 \pm 9.25				Depression	BDD: 90.23 \pm 84.17 months	No comorbidities	NR		
Pang et al., 2020	MDD: 30 (15/15) 35.27 \pm 9.65	Cross-sectional	3 T SW approach (50 TR, 100 s)	HAMD, SHAPS-14, PANAS-N	NA	NA	NR	NR	BD vs. MDD and HC: \uparrow FCS in the thalamus.	Combined static and dynamic FCSs predicted anhedonia severity in BDD patients and negative mood severity in MDD patients.
	HC: 30 (15/15) 34.77 \pm 11.17				Depression	MDD: 74.67 \pm 70.56 months	No comorbidities	NR		
Tang et al., 2022	BD: 38 (19/19) 33.95 \pm 9.83	Cross-sectional	3 T SW approach (50 TR, 100 s)	HAMD	Depression	91.21 \pm 76.01 months	No comorbidities	AD \pm AP \pm MS	BD and MDD vs. HC: \downarrow DRePS in the bilateral OFC extending to the insula, right insula extending to the hippocampus, left hippocampus, right inferior frontal gyrus and thalamus extending to caudate, right caudate, bilateral superior frontal gyrus, and right middle frontal gyrus.	No correlations in BD.
	MDD: 40 (20/20) 35.23 \pm 10.29				Depression	MDD: 69.25 \pm 68.64 Months	NR	NR		
Wang et al., 2019b	HC: 50 (24/26) 33.60 \pm 10.38	Cross-sectional	3 T SW approach (22 TRs) k-means clustering (k = 3) graph theory method	HDRS, YMRS	NA	NA	NR	NR	BD VS. HC: \uparrow time in a state characterized by negative correlations between the SAL, CB, BG, and sensory networks (State 2), \downarrow time in a state characterized by negative correlations between the DMN and other networks (State 3); \uparrow transitions between states, \uparrow dynamic variance in the small-world properties of dFC.	Positive correlation between time spent in State 2 and HDRS in the BD.
	BD: 56 (28/28) 33.23 \pm 10.79				Depression	BDD: 99.14 \pm 86.09 months	No comorbidities	AD + few AP and MS		
Wang et al., 2020	MDD: 98 (38/60) 34.51 \pm 12.15	Cross-sectional	3 T SW approach k-means clustering ROI: SAL, DMN, EXE	HAMD-24, YMRS	NA	NA	NR	NR	BD and MDD vs. HC: \downarrow dFC variability between posterior DMN and right EXE.	NR
	HC: 97 (49/48) 33.92 \pm 14.11				Depression	MDD: 52.63 \pm 64.98	No comorbidities	NR		
Wen et al., 2019	BBD: 51 (24/27) 26.35 \pm 8.79	Cross-sectional	NR SVM	HAMD-24	Depression	NR	No comorbidities	NR	BD vs. MDD: \downarrow variability of dFC in SM	NR
	HC: 50 (20/30) 28.60 \pm 9.87				NA	NA	NR	NR		

(continued on next page)

Table 2 (continued)

Author, year	Subjects number (M/F) Age (years) mean ± SD	Study design	MRI acquisition and dFNC analysis	Clinical scales	Current clinical status	Duration of illness	Comorbidities	Medications	Neuroimaging findings	Correlations with clinical scales
	MDD: 50 (25/25) 35.23 ± 10.29 HC: 50 (24/26) 33.6 ± 10.38				Depression					
Yang et al., 2020	BD: 40 (22/18) 34.43 ± 10.76 HC: 60 (32/28) 31 ± 10.18	Cross-sectional	3 T SW approach (30 TRs) IHC VMHC	HAMD	Depression	NR	No comorbidities	NR	BD vs. HC: ↑ dynamic IHC in the cerebellum, inferior frontal gyrus, temporal, and SM network, ↓ dynamic IHC in the posterior parietal and precuneus.	Correlation between the number of depressive episodes and altered dynamic VMHC in the postcentral gyrus
Zhang et al., 2021	BBD: 27 (16/11) 26.41 ± 8.82 MDD: 21 (9/12) 30.86 ± 11.21 HC: 28 (17/11) 26.07 ± 4.92	Cross-sectional	3 T SW approach ROI: SN	SCID-IV, HAMD-17	Depression	48 ± NR months	No comorbidities	Drug-naïve 4, free 6, medicated 18 Drug-naïve 12, free 3, medicated 6 NR	BD vs. MDD: ↑ dFC in the left prefronto-parietal system.	No correlations in BD.

AD: Antidepressants, AP: Antipsychotics, BD: Bipolar Disorder, BRMS: Bech-Rafarlsen Mania Rating Scale, CWI: Color-Word Interference, dALFF: dynamic amplitude of low-frequency fluctuation, dFC: dynamic functional connectivity, DMN: Default Mode Network, DRePS: Dynamic Regional Phase Synchrony, D-KEFS: Delis-Kaplan Executive Function System, HAMD: Hamilton Depression Scale, HC: Healthy control, HDRS: Hamilton depression rating scale, IHC: Interhemispheric connectivity, MDD: major depressive disorder, MDD: mood stabilizers, NA: not applicable, NR: not reported, PANSS: Positive and Negative Symptoms Scale, PANAS-N: Positive and Negative Affect Scale, ROI: region of interest, SAL: salience, SHAPS: Snaith-Hamilton pleasure, SM: Sensorimotor, SVM: Support Vector Machine, TDA: Temporal Dynamic Analysis, VFT: Verbal Fluency Test, VMHC: Dynamic Voxel mirrored homotopic connectivity, YMRS: Young Mania Rating Scale.

3.4. dFC alterations in BD vs healthy subjects

3.4.1. Global connectivity

A heterogeneous picture of alterations in global dFC was observed in BD. The FCS between the right anterior insula and the right middle occipital gyrus and the left inferior parietal lobule was increased (Pang et al., 2018). Furthermore, in patients with BD in the depressive phase, the dynamic interhemispheric connectivity, defined as the dFC between a given voxel and the corresponding homologous voxel in the contralateral hemisphere, was reduced in the superior parietal lobule, the angular gyrus, the precuneus, and increased in the cerebellum, orbito-frontal cortex, postcentral gyrus, superior temporal gyrus and supplementary motor area. Notably, increased dynamic interhemispheric connectivity in the postcentral gyrus was associated with a greater number of depressive episodes (Yang et al., 2020). When affective status was considered, depressed BD switched more between states and dwelled more in a state characterized by a negative correlation between the SAL, cerebellum, and the subcortical network and the SM, AUD, and VIS, and less in a state characterized by negative correlations between the DMN and other functional networks (Wang et al., 2020). Compared to MDD, unmedicated patients with BD-II showed greater variability in dFC between the dorsal striatal putamen and sensory-motor regions (i.e., left supramarginal area) and the ventral rostral putamen and the parietal cortex (i.e., right inferior parietal lobule), similarly to MDD, and between the dorsocaudal putamen and the motor regions (i.e., precentral gyrus) compared to MDD and HC (Chen et al., 2022). Lastly, a study conducted on euthymic BD reported an increased number of transitions between a high-level cognitive state and a low-level sensory state in BD (Du et al., 2021b).

3.4.2. Default mode network

BD was associated with decreased network switching rate in the DMN (Han et al., 2020). In particular, reduced dFC was present in posterior DMN in depressed patients with BD (Luo et al., 2021), and specifically BD-I (Liang et al., 2020). Also, FCS between DMN (middle temporal gyrus and the postcentral gyrus) and SM (superior temporal gyrus) was reduced during depression relative to euthymia in BD (Liu et al., 2021). In BD-I, the FCS between the two hubs of the DMN (medial prefrontal cortex and posterior cingulate cortex) was less variable over time, indicating greater rigidity and this was associated with reduced cognitive performance (Nguyen et al., 2017).

3.4.3. Executive network

The dFC in the frontal-striatal-thalamic circuit was increased in euthymic BD (Liu et al., 2021) and in depressed BD relative to HC (Tang et al., 2022) and MDD and HC (Pang et al., 2020).

3.4.4. Salience network

Euthymic BD showed increased dFC variability of the right anterior insula. Notably, BD shared a reduced variability between the right ventral anterior insula and the ventrolateral prefrontal cortex with MDD and had the greatest variability of the dFC of the right dorsal anterior insula with temporo-occipital regions compared to MDD and HC (Pang et al., 2018).

3.4.5. Sensory-motor network

A state-dependent increase of FCS between SM and DMN, which was greater in depressed BD relative to euthymic BD relative to euthymic BD and HC, was reported by one study (Liu et al., 2021).

3.4.6. Emotional network

Depressed BD was associated with changes in between-network FCS of the limbic system and precisely increased amygdala-cerebellar and decreased amygdala-postcentral gyral dFC, respectively (Fateh et al., 2020). In addition, depressed BD showed reduced dynamic regional phase synchrony, a measure of instantaneous coherence, in fronto-

Table 3

Selection of studies evaluating dynamic functional connectivity in bipolar disorder and schizophrenia.

Author, year	Subjects number (M/F) Age (years) mean \pm SD	Study design	MRI acquisition and DFNC analysis	Clinical scales	Current clinical status	Duration of illness	Comorbidities	Medications	Neuroimaging findings	Correlations with clinical scales
Das et al., 2020	Psychotic BD: 16 (11/5) 37.0 \pm 9.6 SCZ: 34 (25/9) 41.1 \pm 9.1 HC: 32 (22/10) 33.4 \pm 9.1	Cross-sectional	3 T SW approach ROI: AAL atlas	SSPI, DSST	euthymia	12.1 \pm 8.0 years	NR	NR	SCZ vs. BD: asymmetric left hemispheric \downarrow in FC.	Positive correlation between disorganization and \downarrow left parietal d FC in SCZ.
					clinically stable	9.6 \pm 8.1 years	NR	NR		
					NA	NA	NR	NR		
Du et al., 2017	Psychotic BD: 140 (53/87) 36 \pm 12.57 SCZ: 113 (56/58) 35.57 \pm 12.29 HC: 238 (100/138) 38.15 \pm 12.55	Cross-sectional	NR SW approach ROI: AAL atlas	PANSS	euthymia	NR	No comorbidities	stable medication regimens	22 instances of hypoconnectivity (HC \uparrow BD, BD \uparrow SCZ) involving post-central, frontal, and cerebellar cortices. 34 instances of hyperconnectivity (HC \downarrow SCZ) involving thalamus and temporal cortices. Frontal connectivity: BD similar to HC SCZ vs. HC: altered FC between the left postcentral gyrus and right thalamus. BD vs HC: altered FC between the left postcentral gyrus and left thalamus regions and between right thalamus and left cerebellum. SCZ vs. BD: similarity in the connectivity changes between cuneus and insula, between cuneus and putamen, and between cuneus and supramarginal gyrus. Disorder-common impairments primarily included the \downarrow FCS between thalamus and cerebellum and \uparrow FCS between postcentral gyrus and thalamus.	Negative correlation between hypoconnectivities in postcentral and frontal gyri and PANSS positive and negative scores.
					clinically stable	NR	No comorbidities	stable medication regimens		
					NA	NA	NR	NR		
Du et al., 2020	Psychotic BD: 140 (53/87) 36 \pm 12.57 SCZ: 113 (56/58) 35.57 \pm 12.29 HC: 238 (100/138) 38.15 \pm 12.55	Cross-sectional	NR ROI: AAL atlas	DSM-IV-TR	Depression or euthymia or mania with psychotic symptoms	NR	NR	AP 72.14%, 41.43 CE%, MS 69.29%	BD vs HC: altered FC between the left postcentral gyrus and left thalamus regions and between right thalamus and left cerebellum. SCZ vs. BD: similarity in the connectivity changes between cuneus and insula, between cuneus and putamen, and between cuneus and supramarginal gyrus. Disorder-common impairments primarily included the \downarrow FCS between thalamus and cerebellum and \uparrow FCS between postcentral gyrus and thalamus.	NR
					NR	NR	NR	AP 88.50%, 38.94 CE%, MS 23.01%		
					NA	NA	NR	NR		
Li et al., 2021	BD: 100 (36/64) 24.56 \pm 5.95 SCZ: 150 (59/91) 23.67 \pm 8.77 HC: 210 (86/124) 24.37 \pm 5.74	Cross-sectional	3 T SW approach K-means clustering ROI	HAMD, HAMA, YMRS, BPRS	NR	36.61 \pm 36.09 months	NR	Medicated 65%	SCZ vs. BD: \downarrow connectivity within VIS, SM, SAL and EXE.	NR
					NR	23.27 \pm 34.97 months	NR	Medicated 74%		
					NA	NA	NR	NR		
Long et al., 2020	BD I: 53 (26/27) 25.34 \pm 4.09 SCZ: 66 (38/28) 24.3 \pm 6.1	Cross-sectional	3 T SW approach ROI: AAL atlas	SAPS, SANS, YMRS, HAMD, WAIS-I, WAIS-DS	NR	56.99 \pm 53.91 months	No comorbidities	NR	SCZ and BD vs. HC: \uparrow regional FC variabilities in thalamus and basal ganglia. SCZ vs. HC: \uparrow regional FC	NR
					NR	22.21 \pm 24.97 months	No comorbidities	63 AP		

(continued on next page)

Table 3 (continued)

Author, year	Subjects number (M/F) Age (years) mean \pm SD	Study design	MRI acquisition and DFNC analysis	Clinical scales	Current clinical status	Duration of illness	Comorbidities	Medications	Neuroimaging findings	Correlations with clinical scales
	HC: 66 (28/38) 23.38 \pm 4.42				NA	NA	NR	NR	variabilities in precentral gyrus, postcentral gyrus, inferior parietal lobule, hippocampus and amygdala, \downarrow regional FC variabilities in the superior frontal gyrus. SCZ vs. BD: \downarrow regional FC variabilities in the posterior cingulate gyrus. SCZ and BD vs. HC: \uparrow variability for inter-network FC between the SM and thalamus. SCZ vs. HC: \uparrow variabilities of both intra-network and inter-network FC in SM, VIS and subcortical networks.	
Rashid et al., 2014	BD: 38 (18/20) 38.96 \pm 10.90 SCZ: 60 (47/13) 35.85 \pm 12.01 HC: 61 (33/28) 35.44 \pm 11.57	Cross-sectional	3 T SW approach (22 TRs, 33 s) K-means clustering (k = 5)	NR	euthymia clinically stable	NR NR	NR NR	NR NR	SCZ vs. BD vs. HC: \uparrow differences in SCZ from HC than BD SCZ vs. BD: differences in states of connectivity involving frontal-parietal regions	NR
Zhu et al., 2020	BD: 44 (19/25) 35.0 \pm 9.1 SCZ: 47 (12/35) 36.5 \pm 8.8 HC: 115 (53/62) 31.1 \pm 8.6	Cross-sectional	3 T Functional stability	DSM-IV, SAPS, SANS, HAMD, YMRS	NR NR	NR NR	NR NR	NR NR	SCZ vs. HC: \uparrow functional stability in the bilateral inferior temporal gyrus and \downarrow stability in the bilateral calcarine sulcus and left insula. BD vs. HC: \downarrow local stability in the left inferior temporal gyrus. SCZ and BD vs. HC: \uparrow functional stability in the left inferior temporal gyrus. SCZ vs. BD: \downarrow functional stability in the right calcarine sulcus.	No significant correlations between functional stability and clinical symptoms.

AAL: Automated Anatomical Labeling, AD: Antidepressants, AP: Antipsychotics, ATT: attentional, BP: Bipolar Disorder, BPP: Bipolar disorder with Psychosis, BPRS: Brief Mania Rating Scale, dFC: Dynamic Functional Connectivity, DMN: Default Mode Network, DSST: Digit Symbol Substitution Test, FC-rs: Functional connectivity resting state, HAMD: Hamilton Depression Scale, HAMA: Hamilton Anxiety Scale, HC: Healthy Control, MD: mood stabilizer, NA: not assessed, NR: not reported, PANSS: Positive and Negative Symptoms Scale, ROI: regions of interest, SAPS: Assessment of Positive Symptoms, SANS: Assessment of Negative Symptoms, SCZ: Schizophrenia, SSPI: Sing and Symptoms of Psychiatric Illness, WAIS-I: Wechsler Adult Intelligence Scale, WAIS-DS: Wechsler Adult Intelligence Scale Digit Symbol, YMRS: Young Mania Rating Scale.

striato-limbic areas (Tang et al., 2022).

3.5. dFC differences between SCZ and BD

Studies comparing SCZ and BD indicated greater dysconnectivity in SCZ relative to BD, with a pattern of decreased within-network dFC in VIS, SM, SAL and EXE, increased dFC between the VIS and the EXE, SAL

and limbic networks, and decreased dFC between the SAL and EXE, DMN and SM, and EXE and DMN (Li et al., 2021). SCZ had more widespread dFC changes relative to BD, involving increased FC variability in the SM, VIS, attention, limbic and subcortical areas at the regional and network levels, as well as decreased regional FC variabilities in the DMN areas (Long et al., 2020). In line with this, a similar aberrant FC pattern was reported in DMN, VIS, SM, and EXE in SCZ and

Table 4
Processing steps for the calculation of dynamic functional connectivity.

Signal extraction			
Method	Statistics	Signal	Pros and cons
Independent component analysis (ICA)	Multivariate	Time courses of several independent components from the mixing matrix	Pros: effective at a group scale, no prior spatial assumptions Cons: a priori number of components
Seed-based functional connectivity	Univariate (correlation)	Representative time course from a single ROI	Pros: effective at a subject level Cons: a priori selection of seeds
Regional Homogeneity	Univariate (KCC)	Time course similarity among neighboring voxels	Pros: no prior spatial assumptions Cons: local measure (classically 27 voxels)
Low-frequency fluctuations (ALFF, fALFF)	Univariate	Low-frequency spectrum of the voxel time course	Pros: no prior spatial assumptions Cons: limited to low-frequency band
Mirrored homotopic connectivity	Univariate (correlation)	Time course of mirror areas	Pros: interhemispheric connectivity estimation Cons: only homotopic regions are considered
dFC calculation			
Method		Signal	Pros and cons
Sliding window		Voxel-wise correlation maps	Pros: Easy to implement Cons: window size (too large does not detect small fast changes; too small does not capture variability) Low-pass filtering due to the size
Filtered bank on connectivity domain		Connectivity matrices	Pros: no low-pass filter Cons: window size; high-frequency noise effects
Dynamic directional functional domain connectivity		domain-level "dynamic states"	Pros: domain-level Cons: window length and domain assignment
Weighted average of shared trajectory		Trajectory of time courses	Pros: short window length Cons: nonlinear mixing
Estimation of connectivity states			
Method		Description	Pros and cons
k-means clustering		Algorithm to partition data based on the nearest means (centroid)	Pros: easy to implement, scales to large data sets Cons: local minima; influenced by noise
Principal component analysis (PCA)		Decomposition in linear orthogonal combinations of FC patterns	Pros: removes correlated features and overfitting Cons: reduced variables become less interpretable, information loss
Spatial and temporal independent component analysis (s-ICA)		Decomposition in linear spatially or temporally combinations of FC patterns	Pros: effective at a group scale, no prior spatial assumptions Cons: a priori number of components
Affinity propagation		Pairwise similarity that is propagated	Pros: no a priori selection of the number of clusters Cons: difficult to scale to large datasets
Statelets		Similarity metric for motifs comparison	Pros: estimation of brief, repetitive co-

Table 4 (continued)

Signal extraction			
Method	Statistics	Signal	Pros and cons
		(earth mover distance)	fluctuations Cons: high time complexity and parameter tuning

ALFF: Amplitude of low frequency fluctuations, dFC: Dynamic functional connectivity, fALFF: Fractional amplitude of low frequency fluctuations; FC: Functional connectivity, KCC: Kendall's coefficient of concordance, ROI: region of interest.

BD, with a greater magnitude of changes in SCZ relative to HC (Rashid et al., 2014). Parieto-parietal inter-hemispheric network dFC was greater in both SCZ and BD in the right hemisphere, and in BD only in the left hemisphere, respectively, compared to HC (Das et al., 2020). Furthermore, an increase in functional stability in VIS (i.e., calcarine sulcus) was reported in BD relative to SCZ, indicating a higher concordance of dynamic FC over time in these patients (Zhu et al., 2020). When compared within the bipolar-schizophrenia spectrum, a reduced dFC fronto-parieto-cerebellar circuit with increased dFC in corticothalamic networks was observed, and the magnitude of this dysconnectivity increased from HC to BD, schizoaffective disorder (SAD), and SCZ. SCZ, BD, and SAD shared a decrease in FCS between the thalamus and cerebellum and an increase in FCS between the postcentral gyrus and the thalamus (Du et al., 2017). A follow-up study showed that BD and SCZ had similar connectivity changes between VIS (i.e., cuneus) and the insula, the putamen, and the supramarginal gyrus (Du et al., 2020).

3.6. Brain-behavior correlations

3.6.1. PANSS positive

In SCZ, the PANSS positive score was associated with the variability of dFC and cross-domain mutual information (Dong et al., 2019; Salman et al., 2019) and sample entropy (Jia and Gu, 2019) of the VIS, in addition to dynamic time-varying measures of SAL (He et al., 2021; Supekar et al., 2019). Furthermore, a correlation was observed between PANSS positive scores and FCS of the left thalamus (Luo et al., 2020) and temporal regional efficiency in the left inferior orbitofrontal gyrus (Sun et al., 2019). In BD, SAD, and SCZ, hypoconnectivity between post-central and frontal gyri was negatively correlated with PANSS positive scores (Du et al., 2017).

3.6.2. PANSS negative

In SCZ, the PANSS negative scores were correlated with the variability of dFC and temporal regional efficiency (Deng et al., 2019; Sun et al., 2019), and the entropy (Jia and Gu, 2019) of VIS and abnormal FC variability (Dong et al., 2019). Additionally, an association was also observed between PANSS negative and FCS in the right insula and the left orbital inferior frontal gyrus (Luo et al., 2020) and the left cerebellum crus 1 (Wang et al., 2019a). Moreover, negative symptom severity was associated with the probability of transition from a state with predominant anterior-to-posterior DMN (lower precuneus/posterior cingulate cortex and higher anterior cingulate cortex) FC relative to a state with reverse pattern (higher precuneus/posterior cingulate cortex and lower anterior cingulate cortex) (Sendi et al., 2021b). Dwelling longer in a state characterized by sparse and weak connectivity predicted PANSS negative scores, with reduced DMN and VIS dFC predicting greater attention domain impairment (Yang et al., 2022).

In a study conducted in a small sample of adolescent-onset SCZ, reduced dFC between the left middle temporal gyrus and the left extrastriate visual area predicted increased emotional withdrawal evaluated with item 2 of PANSS negative (Sun et al., 2021). Lastly, hypoconnectivities linking postcentral and frontal gyri were negatively correlated with the PANSS negative scores in BD, SAD, and SCZ (Du

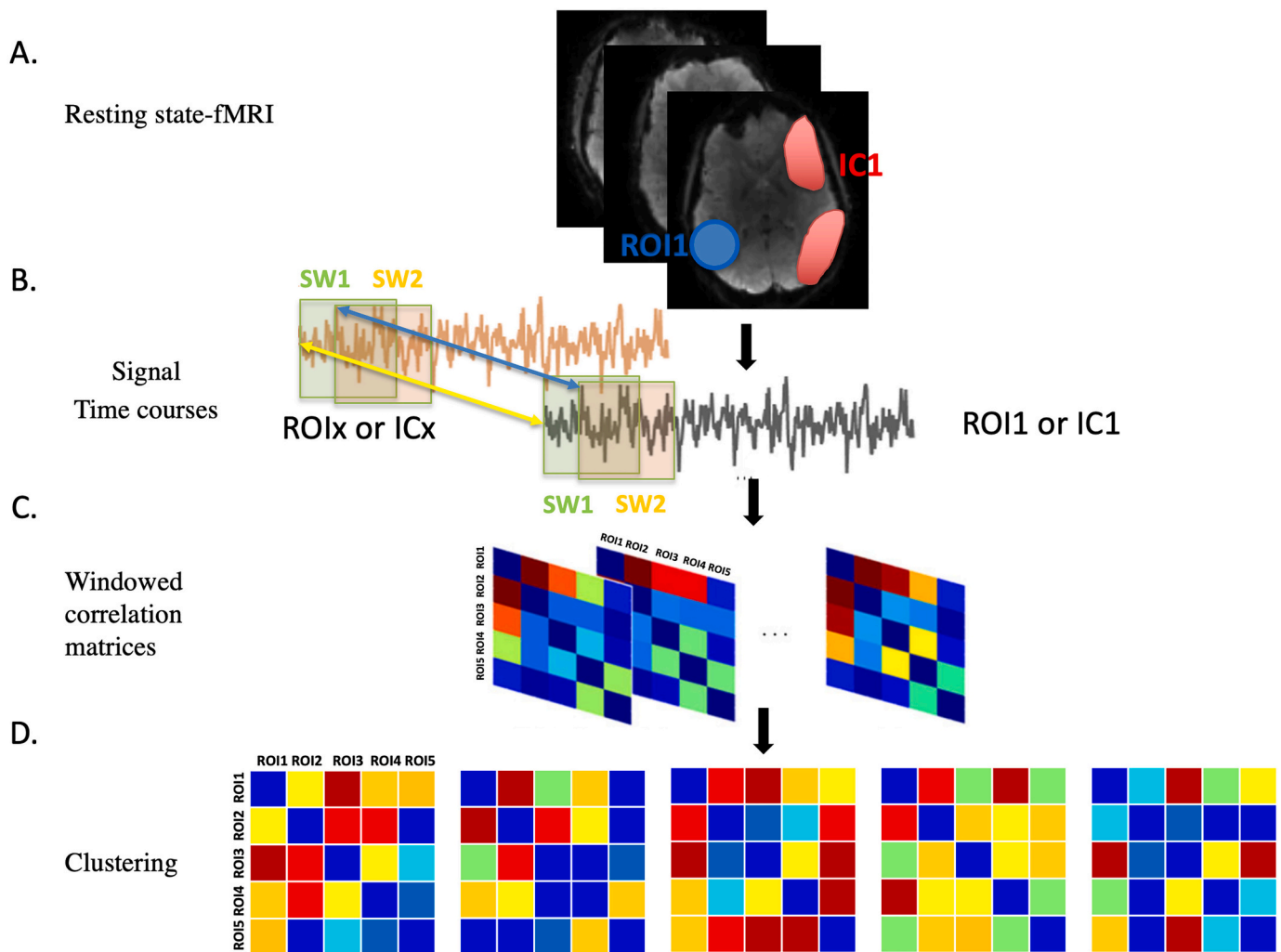


Fig. 2. Estimation of functional network connectivity starts from A) the time series of regions of interest or independent component analysis or other measures from resting state fMRI data; B) the signal is then analyzed across several sliding windows to calculate the correlation between signals that is C) entered in correlation matrices; D) these matrices are clustered in connectivity states.

et al., 2017).

3.6.3. PANSS general

Scores of general psychopathology were correlated with dynamic measures of the nodes of the VIS (Jia and Gu, 2019) VIS, SM and thalamus (Dong et al., 2019), left inferior orbitofrontal gyrus (Sun et al., 2019), right supramarginal gyrus (Wang et al., 2019a), right amygdala and left inferior parietal gyrus (Jia et al., 2017).

3.6.4. ANSS total

The FCS of the cortico-thalamic circuits (i.e., the bilateral insula, left thalamus, and left paracentral lobule) (Luo et al., 2020), of temporal (i.e., right amygdala and left temporal pole) (Sun et al., 2019), and striato-parietal networks (i.e., right supramarginal gyrus and right putamen) (Wang et al., 2019a), reduced dALFF of the SAL-EXE connection (He et al., 2021), and increased variability of dFC of the frontal-amygdala connection (Yue et al., 2018) were associated with a higher PANSS total score, thus supporting the dysconnectivity hypothesis of SCZ (Yue et al., 2018). Additionally, the overall symptom severity was associated with the greater probability of transitioning from a state with predominant anterior-to-posterior DMN (lower precuneus/posterior cingulate cortex and higher anterior cingulate cortex) FC relative to a state with reverse pattern (higher precuneus/posterior cingulate cortex and lower anterior cingulate cortex) (Sendi et al., 2021b). The FC variability of VIS

(Deng et al., 2019) and VIS, SM, and thalamus (Dong et al., 2019) was associated with a higher PANSS total score.

The correlations between PANSS scores and dFC measures are summarized in Table 5.

3.6.5. Other symptom scales

In SCZ, trait hallucination proneness over one year showed a significant association with dwell times in a state characterized by strong positive FC within the DMN and negative FC between the DMN and the insula (Weber et al., 2020), while hallucination severity measured with BPRS was positively correlated with the temporal instability of lateral occipital cortex connectivity (Li et al., 2020). Additionally, illness duration was associated with the entropy of the VIS (i.e., left superior occipital gyrus) (Jia and Gu, 2019), cortico-limbic networks (i.e., right amygdala, right superior orbital frontal gyrus, and left inferior parietal gyrus) (Jia et al., 2017). In depressed BD, depression severity (HAMD score) was positively correlated with the dFC between the right anterior insula and inferior parietal lobule (Pang et al., 2018) and with dwelling in a state with decreased FC between DMN, SAL, and EXE (Wang et al., 2019b). Moreover, in depressed BD, the abnormal dynamic FCS in the frontal-striatum-thalamic circuit predicted anhedonia measured with the Snaith-Hamilton Pleasure Scale (Pang et al., 2020). Disorganization evaluated with the SSPI was associated with dFC in the SCZ, but not in BD (Das et al., 2020). The correlations between clinical scales and dFC

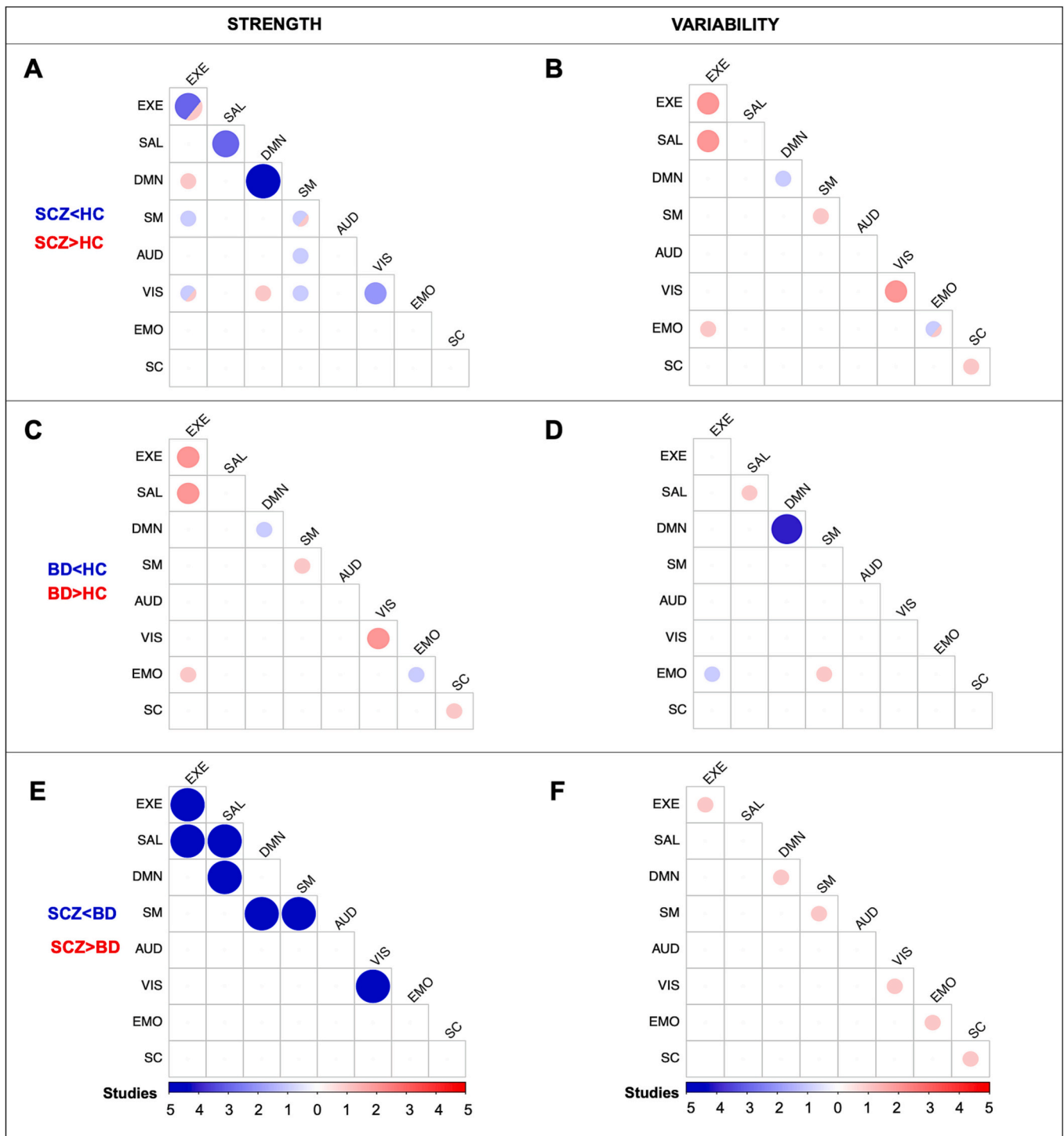


Fig. 3. Dynamic Network Functional connectivity (dFC) changes in schizophrenia (SCZ) and bipolar disorder (BD). Correlograms display differences in functional connectivity strength in SCZ (A), in BD (C) relative to healthy controls (HC) and between diagnosis (E) and in the dFC variability for SCZ (B), BD (D) relative to healthy controls (HC) and between diagnosis (F) for each cross-correlation in a lower triangular matrix. The color intensity and circle size reflect the number of studies reporting a difference, with red and blue color indicating greater and reduced dFC in the diagnostic groups relative to HC in the first two rows and in SCZ relative to BD in the last row, respectively. The color bar indicates the number of studies reporting a difference. In a circle, a sector with different color indicates contrasting results and each color reflects the number of studies supporting each direction. EXE, executive; SAL, salience; DMN, default mode network; SM, sensory-motor; AUD, auditory; VIS, visual; EMO, emotional; SC, subcortical. (For interpretation of the references to color in this figure legend, the reader is referred to the web version of this article.)

measures are summarized in [Table 5](#).

3.6.6. Cognitive performances

Four studies explored the relationship between dFC measures and

cognitive performance in SCZ and BD ([Table 6](#)). In SCZ, dwell time in a state with positive FC within the middle temporal gyrus and between the middle temporal gyrus with other regions predicted visual learning memory ([Sendi et al., 2021a](#)). The variability of FC in cortico-limbic

circuits (i.e., amygdala-medial prefrontal cortex) was associated with poorer performance on the digit symbol coding task (Yue et al., 2018), while the temporal instability of the lateral occipital cortex connectivity predicted higher switching costs during task performance in SCZ (Li et al., 2020). In BD, reduced connectivity variability within the DMN was associated with slower processing speed and impaired set-shifting (Nguyen et al., 2017).

3.7. Effect of medications on dFC

Four studies explored the effects of second-generation antipsychotics on dFC in SCZ and they all described a normalizing effect on dFC and clinical symptoms. Unfortunately, the sample size of these studies was considerably smaller compared to most cross-sectional studies. Two longitudinal trials focused on risperidone (Duan et al., 2020; Lottman et al., 2017). The first employed risperidone at a dosage of 4–6 mg/day for 8 weeks in antipsychotic-naïve first-episode patients with SCZ and observed a normalization of the dFC variance of the abnormal connections (Duan et al., 2020), while the second showed a normalization of mean dwell times in a sparsely connected state with a dosage of 4.4 mg/day after 6 weeks (Lottman et al., 2017). In both studies, the treatment also resulted in clinical improvement. Wang et al. (2021) explored dFC after 12 weeks of treatment with various atypical antipsychotics, including olanzapine, risperidone, paliperidone, ziprasidone, quetiapine, amisulpride, and aripiprazole in monotherapy (62.5%) or in combination (37.5%) and showed that, compared with HC, SCZ presented more unstable brain states, which normalized to some extent after antipsychotic treatment. Furthermore, in this case, antipsychotic treatment was associated with a decrease in PANSS scores (Wang et al., 2021). Lastly, after 8 weeks of various antipsychotic treatments, including paliperidone, clozapine, risperidone, olanzapine, aripiprazole, and quetiapine, a significant increase in the symptomatic improvement-related occurrence of a dFC state characterized by greater inter-network integration was observed. Furthermore, the reduction in symptoms was correlated with increased FC variability in the connections within the DMN and between the AUD, EXE, and cerebellar network to other networks (Zhang et al., 2021).

4. Discussion

Our systematic review aimed at summarizing all available evidence on dFC alterations at resting state in SCZ and BD and their association with psychiatric symptoms and behavior. We found a global alteration of dFC in SCZ, while a more heterogeneous picture of altered dFC was observed in BD. However, in both disorders, dysfunction of the triple network involved in the performance of goal-directed behavior emerged. A direct comparison between SCZ and BD confirmed a predominant pattern of dysconnectivity in the triple network in SCZ. Psychopathological measures showed an association with dFC metrics in almost all the studies on SCZ, with positive and negative symptoms demonstrating an association with abnormal dFC. Remarkably, dFC alterations were normalized after antipsychotic treatment in responders.

4.1. Schizophrenia

Overall, the findings of our review show a consistent pattern of dFC alterations in SCZ compared to HC, involving abnormal FCS and an increased dwell time and a number of transitions to states characterized by weaker connectivity within and between all major resting-state networks.

Significant progress in the neuroimaging field in recent decades has provided robust evidence to the so-called “dysconnectivity” theory, postulated to explain the core psychopathological characteristics of SCZ. First described in the 1990s, this theory was based on the observation of abnormal functional integration between anatomically distinct brain regions (Friston and Frith, 1995; Stephan et al., 2009) at the core of

symptomatology in SCZ. Importantly, SCZ is characterized by both global dysconnectivity, as demonstrated by global signal abnormalities, and alterations at the topographic level in lower-order sensory and higher-order cognitive regions that may underlie sensory and cognitive symptoms (Yang et al., 2014; Zhang and Northoff, 2022). Accordingly, a consistent pattern of dFC alterations in the triple network has been suggested to play a prominent role in the pathogenesis of SCZ (Dong et al., 2018; Menon, 2011). Interestingly, structural and functional alterations in SAL have been commonly associated with impaired attribution of salience to stimuli, which, in turn, is associated with delusions and hallucinations in SCZ (Palaniyappan et al., 2011). Furthermore, altered FC between SAL, EXE, and DMN has been associated with positive and negative symptoms (Hare et al., 2019b; Manoliu et al., 2014). In our review, alterations in dFC involving areas of the triple network appeared to be associated with psychiatric symptoms in SCZ (Dong et al., 2019; He et al., 2021; Luo et al., 2020; Salman et al., 2017; Sun et al., 2019). Among these, Supekar et al. (2019) showed a positive association between the lack of dynamic engagement of the SAL with the EXE and DMN and disorganized thought (Supekar et al., 2019). Overall, our results suggest that patients with SCZ present a reduction in dynamic connectivity metrics in the triple network, which may underlie psychotic symptoms for altered salience attribution, negative symptoms for altered DMN persistence, and cognition for impairment of EXE connectivity. In addition, abnormalities in dFC were reported in sensorimotor circuits, particularly in the VIS (Deng et al., 2019), AUD (Geng et al., 2020), and SM (Sambataro et al., 2021b), suggesting that altered FC metrics in these areas could be associated with deficits in the processing of external stimuli, which may lead to psychotic symptoms (Kubera et al., 2019; Thoma et al., 2016). In particular, abnormalities in the VIS and AUD pathways have been commonly reported in SCZ (Harvey et al., 2011; Kaufmann et al., 2015), and appear to be associated with hallucinations and negative symptoms (Orliac et al., 2017).

Interestingly, several studies have shown a relationship between changes in SM network dynamics and psychopathological measures, such as PANSS total (Deng et al., 2019; Dong et al., 2019), general (Dong et al., 2019; Jia and Gu, 2019) and negative scores (Deng et al., 2019; Jia and Gu, 2019; Wang et al., 2019a). Furthermore, changes in dFC in sensory networks showed a correlation with positive symptoms evaluated with PANSS (Dong et al., 2019; Jia and Gu, 2019; Salman et al., 2017; Sun et al., 2019), as well as with hallucination severity measured with BPRS (Li et al., 2020). These results align with the spatiotemporal model of psychopathology proposed by Northoff and Duncan (Northoff, 2015; Northoff and Duncan, 2016), according to which temporal and spatial changes in spontaneous brain activity affect cognitive and affective processing in SCZ. In particular, abnormalities in the SM and the sensory networks dFC could be associated with altered perceptions of spatial relationships with respect to the body and the environment in patients with SCZ, which might lead to delusions and hallucinations. Furthermore, as previously demonstrated in depression (Northoff, 2016), affective and cognitive symptoms such as anhedonia could be the phenotypic manifestation of spatiotemporal disturbances of the activity of the resting state that in SCZ appear to be prevalent in the VIS network, frontal areas, insula, and cerebellum.

Interestingly, dFC abnormalities have also been reported in individuals at genetic risk for SCZ (Braun et al., 2016). Meta-analytic evidence from task-based fMRI studies has shown that unaffected relatives of SCZ present a pattern of functional abnormalities involving the cortico-striato-thalamic network (Cattarinussi et al., 2022), while the few available rs-fMRI studies showed alterations in the prefrontal, thalamic, limbic, and SAL networks (Li et al., 2015; van Leeuwen et al., 2021; Xi et al., 2020). Abnormal dFC in subjects at risk for SCZ suggests that these alterations are not related to the pathology itself but may be a risk phenotype of the disorder (intermediate phenotype).

Finally, studies investigating the effect of antipsychotics on dFC in SCZ showed a normalization of the metrics of dFC after treatment, which was accompanied by a symptomatic improvement (Duan et al., 2020;

Table 5

Associations between clinical scales and dFC measures in schizophrenia and bipolar disorder.

Clinical scales		Associations between clinical scales and dFC measures
PANSS positive	SCZ	- negative correlation with the variability of region-to-whole-brain FC in the right lingual gyrus (Dong et al., 2019) - negative correlation with dFC of insula within SAL (He et al., 2021) - positive correlation with sample entropy of the right inferior occipital gyrus (Jia and Gu, 2019) - positive correlation with FCS of the left thalamus (Luo et al., 2020) - positive correlation with VIS-FRN vs. VIS-DMN CDMI (Salman et al., 2019) - positive correlation with temporal regional efficiency in the left inferior orbitofrontal gyrus (Sun et al., 2019) - positive correlation with SAL-centered time-varying cross-network interactions (Supekar et al., 2019) - negative correlation with the hypoconnectivities linking the postcentral and frontal gyri (Du et al., 2017)
	BD and SCZ	
PANSS negative	SCZ	- positive correlations with the FC variability of the right fusiform gyrus (Deng et al., 2019) - positive correlation with the variability of region-to-whole-brain FC in the right insula (Dong et al., 2019) - positive correlation with sample entropy of the right middle occipital gyrus (Jia and Gu, 2019) - negative correlation with the FCS of the bilateral insula and positive correlation with the FCS of the left orbital inferior frontal gyrus (Luo et al., 2020) - positive correlation with the probability of transitioning from a state with predominant anterior-to-posterior DMN FC relative to a state with a reverse pattern (Sendi et al., 2021b) - negative correlation with temporal regional efficiency in the right precuneus and left temporal pole (Sun et al., 2019) - negative correlation with the dFC between the left middle temporal gyrus and the visual area (Sun et al., 2021) - negative correlation with FCS in the left cerebellum crus 1 (Wang et al., 2019a) - positive correlation with dwell time in a state characterized by sparse and weak connectivity (Yang et al., 2022) - negative correlation with the hypoconnectivities linking the postcentral and frontal gyri (Du et al., 2017)
	BD and SCZ	
PANSS general	SCZ	- negative correlation with the variability of region-to-whole-brain FC in the right lingual gyrus, bilateral precentral gyrus, and thalamus (Dong et al., 2019) - positive correlation with the sample entropy of the right amygdala and left inferior parietal gyrus (Jia et al., 2017) - positive correlation with sample entropy of the right inferior occipital gyrus (Jia and Gu, 2019) - positive correlation with the temporal regional efficiency in the left orbitofrontal gyrus (Sun et al., 2019) - negative correlation with FCS in the right supramarginal gyrus (Wang et al., 2019a)
PANSS total	SCZ	- positive correlation with the FC variability of the right fusiform gyrus (Deng et al., 2019) - negative correlation with FCS of the left insula, positive correlation with FCS of the left thalamus, negative correlation with FCS of the left paracentral lobule (Luo et al., 2020) - negative correlation with FCS of the striato-parietal networks (Wang et al., 2019a) - negative correlation with the connectivity between dALFF in SAL and EXE (He et al., 2021) - negative correlation with temporal regional efficiency in the right amygdala and left temporal pole (Sun et al., 2019) - positive correlations with FC variability of amygdala – prefrontal cortex (Yue et al., 2018) - positive correlation with the probability of transitioning from a state with predominant anterior-to-posterior DMN FC relative to a state with a reverse pattern (Sendi et al., 2021b) - negative correlation with the FC variability of VIS, SM, and thalamus (Dong et al., 2019)
BPRS HAM-D	SCZ BD	- positive correlation between hallucination severity and temporal instability of lateral occipital cortex dFC (Li et al., 2020) positive correlation between: - depression severity and the dFC between the right anterior insula and the inferior parietal lobule (Pang et al., 2018) - dwell time in a state with decreased FC between DMN, SAL, and EXE (Wang et al., 2019b)
SHAPS SSPI	BD SCZ	- positive correlation between FCS in the frontal–striatum–thalamic circuit and anhedonia in depressed BD (Pang et al., 2020) - positive correlation between parietal dFC and disorganization (Das et al., 2020)

BD: Bipolar Disorder, BPRS: Brief Psychiatric Rating Scale, dFC: Dynamic functional connectivity, CDMI: Cross-domain mutual information, DMN: Default mode network, EXE: Executive network, FC: Functional connectivity, FCS: Functional connectivity strength, FRN: Frontoparietal network, HAM-D: Hamilton Depression Scale, LOC: Lateral occipital cortex, PANSS: Positive and Negative Syndrome Scale, SAL: Salience network, SCZ: Schizophrenia, SHAPS: Snaith-Hamilton Pleasure Scale, SSPI: Sign and Symptoms of Psychiatry illness, SM: Sensorimotor network, VIS: Visual network.

Lottman et al., 2017; Wang et al., 2021; Zhang et al., 2021). It is plausible that dFC abnormalities may reflect disorganized patterns of neuronal activity that could result in the inability of patients to reside in globally coherent states, leading to an impaired ability to perceive, process, and filter out external information. Antipsychotic medications, which decrease neurotransmitter hyperactivity, might attenuate aberrant brain dynamics and result in a decrease in symptoms (see below).

4.2. Bipolar disorder

A more heterogeneous picture is derived from studies conducted in patients with BD. Here, previous findings at rest commonly reported topographical alterations in the motor cortex and hippocampus that vary with mood phase and reflect behavioral and cognitive symptoms, while the global signal does not appear to change (Zhang and Northoff, 2022). The abnormalities of the dFC involved a wide range of cortical and subcortical areas, including frontal areas, limbic lobe, basal ganglia, and thalamus, along with large brain networks, such as DMN, EXE, SAL, and SM. Our results are in line with static rs-fMRI investigations that showed that BD was characterized by hypo and hyperconnectivity within the DMN, affective, EXE, ventral attention, SM and thalamic

networks (Gong et al., 2021). In particular, in BD we found that the anterior insula, which is a key node of the SAL, had greater connectivity to the inferior parietal cortex, a node of the EXE, and reduced connectivity to the right ventrolateral FPC, which is another important region of this network for the control of cognition and impulsivity. Additionally, the DMN showed reduced integrity and modulation both in terms of lower network switching and reduced connectivity between its sub-networks, reduced dALFF, and altered interplay with anticorrelated networks, including EXE and SM. Abnormal thalamocortical connectivity may be a part of EXE dysfunction and may contribute to emotional dysregulation (Ramsay, 2019), which is a prominent feature of this disorder (Miola et al., 2022). Altered connectivity of the SAL can result in impaired cognition-emotion interaction and therefore contribute to the well-known mood and cognition impairments reported in BD (Ellard et al., 2019). Furthermore, altered amygdala connectivity has been extensively studied in BD for its role in emotional processing and for its widespread interaction with brain networks (Rey et al., 2021).

Abnormal connectivity of the amygdala may contribute to the pathogenesis of the emotional and behavioral symptoms that are present in BD (Luo et al., 2018) by: 1) increased connectivity with the cerebellum, which has been implicated not only in sensorimotor function but

Table 6

Associations between cognition and dFC measures in schizophrenia and bipolar disorder.

Group	Cognitive tests	Associations between cognition and dFC measures
SCZ	visual learning memory	- dwell time in a state with positive FC within the middle temporal gyrus and between the middle temporal gyrus with other regions predicted visual learning memory performances (Sendi et al., 2021a)
	digit symbol coding task	- variability of FC in cortico-limbic circuits was associated with poorer performance on the digit symbol coding task (Yue et al., 2018)
	switching costs	- temporal instability of lateral occipital cortex connectivity predicted higher switching costs during task performance (Li et al., 2020)
BD	processing speed and set-shifting	- reduced FC variability within the DMN was associated with slower processing speed and impaired set-shifting (Nguyen et al., 2017)

BD: Bipolar Disorder, DMN: Default mode network, FC: Functional connectivity, SCZ: Schizophrenia.

also in emotion and motivational processing and in several psychiatric disorders (Phillips et al., 2015); 2) reduced connectivity with the somatosensory cortex (postcentral gyrus) that could be responsible for the interaction between emotion and motor control and its subjective experience (Toschi et al., 2017). Remarkably, these functional coupling changes were also present in studies that focused only on BD-I, which is more closely related to SCZ, suggesting partial shared pathophysiological mechanisms for these disorders (Trevisan et al., 2022). These heterogeneous results could be explained by the manifold clinical characteristics of patients with BD, both in terms of mood state (i.e., depression, euthymia, mania), presence/absence of psychotic symptoms and duration of the disease. Interestingly, half of the studies that explored the correlations between dFC metrics and psychopathology observed an association with depressive symptoms evaluated with HAMD (Pang et al., 2018; Wang et al., 2019b) and the severity of anhedonia (Pang et al., 2020), while the others did not.

4.3. Disorder-specific changes

Investigations comparing dFC in SCZ and BD showed that these disorders present some commonalities, however FC alterations were more pronounced in SCZ compared to BD. Notably, studies exploring the association between psychopathology and dFC in BD and SCZ showed that dynamic FC parameters in SCZ were correlated with the disorganization evaluated with the SSPI scale in the SCZ group, while no correlations were observed in the BD group (Das et al., 2020). Interestingly, a correlation was observed between PANSS scores and dFC in BD, SAD, and SCZ (Du et al., 2017). Furthermore, dFC metrics were also correlated with cognitive performance in SCZ and BD, suggesting that brain dynamics could be involved not only in the development of psychopathology but also in cognition.

4.4. Altered connectivity and signaling pathophysiological models

At the level of brain circuits, the dynamics of functional connectivity can arise from changes in local cortical states that can interact with remote regions within large-scale networks (Hutchison et al., 2013). Additionally, subcortical circuits, including subthalamic and brainstem regions, could affect the reconfiguration of these brain networks by modulating neurotransmitter signaling systems. Dopamine has been associated with the dynamics of brain networks (Sambataro et al., 2009) for its role in stabilizing cortical responses through the modulation of cortical pyramidal neurons and GABA-inhibitory interneurons. Furthermore, GABA can modulate the frequency of membrane oscillations and result in increased synchronization within large-scale

networks (Seamans and Yang, 2004). Increased presynaptic dopamine signaling has been implicated in SCZ, in the so-called “dopamine hypothesis”, and similarly, albeit of a small magnitude, increased D2/D3 availability and striatal dopamine amino transporter levels have been reported in BD (Ashok et al., 2017). The normalizing effects of antipsychotics that are mostly D2 antagonists seem to corroborate these results.

Furthermore, glutamate signaling (particularly *N*-methyl-D-aspartate, NMDA) has also been implicated in modulating brain dynamics and in SCZ. Braun et al. (2016) showed that, during working memory processing, dextromethorphan, an NMDA-receptor antagonist, can increase network flexibility, a measure of the ability to reconfigure a node within a network, which suggests temporal disorganization of the community structure of the brain (Braun et al., 2016). Similar hyperflexibility was also found in SCZ in the same study. In particular, altered glutamatergic signaling with hypoactivity of the NMDA system in excitatory pyramidal cortical cells and in fast-spiking GABA inhibitory interneurons can affect the synchrony of brain oscillations and their discharge, ultimately translating into reduced stability of brain networks (Uhlhaas and Singer, 2010), and can result in positive, negative, and cognitive symptoms of SCZ (Merritt et al., 2013). Moreover, converging evidence from pre-clinical and clinical studies suggests an increased activity of NMDA in BD, with mood stabilizers modulating the glutamatergic signaling (Fountoulakis, 2012). Pharmacological studies with NMDA antagonists, including ketamine, memantine, and magnesium, have also shown some efficacy in BD depression, although further studies are needed to confirm these results (Delfino et al., 2020). Finally, antipsychotics can modulate NMDA activity and this effect can contribute to their clinical effects (Choi et al., 2009). In general, alterations in dopamine and glutamate signaling can alter dFC and contribute to the pathophysiology of SCZ and BD.

Overall, brain connectivity at rest is not static but oscillates over time across several brain states, which can be defined as spatial patterns of signals that are stable for a certain period of time. The study of dFC is complex as the time scale of the phenomena that occur in the brain can be highly variable, the number of states is unknown, and they can be intertwined and interact with each other. Furthermore, cross-frequency coupling may drive the self-organized dynamics of brain states with low-frequency oscillations modulating the synchronization patterns of faster rhythms (Vanhatalo et al., 2004). Recent approaches have tried to unravel the interaction between brain states and have considered the coexistence of multiple states at a specific time point rather than an all-or-nothing phenomenon (Miller et al., 2016c). These achievements have contributed to a better understanding of SCZ and BD in terms of brain dynamics. Future studies on the physiology, reliability, and replicability of dFC indexes are needed to create gold standard measures for this novel field, thus allowing the comparability across studies, and more thorough analyses of the molecular and electrophysiological correlates of these phenomena (Hutchison et al., 2013).

4.5. Limitations

The results of this review must be interpreted in light of some limitations. First, there was considerable heterogeneity in the image acquisition parameters and dFC techniques used by the included studies. Second, the characteristics of the patients differed between the studies, increasing the ecological validity of this study, but, at the same time, contributing to the heterogeneity of our findings. Third, the majority of patients were taking psychotropic medications, which could have influenced our results.

5. Conclusions

In conclusion, a pattern of abnormal dFC was observed in SCZ, involving mainly the EXE, SAL, DMN, and sensorimotor circuits, and these alterations are associated with psychopathological features such as

hallucinations and delusions. In BD, a mixed picture of altered dFC was observed, with only some studies reporting an association with affective symptoms. Alterations in dFC have also been observed in unaffected relatives of SCZ, but not in individuals at clinical risk of psychosis. Lastly, antipsychotic treatment, when effective in relieving psychiatric symptoms, seems to play a normalizing role in dynamic abnormalities, thus suggesting a potential avenue for developing effective treatments.

Declaration of Competing Interest

The authors declare that they have no known competing financial interests or personal relationships that could have appeared to influence the work reported in this paper.

Appendix A. Supplementary data

Supplementary data to this article can be found online at <https://doi.org/10.1016/j.pnpbp.2023.110827>.

References

- Allen, E.A., Damaraju, E., Plis, S.M., Erhardt, E.B., Eichele, T., Calhoun, V.D., 2014. Tracking whole-brain connectivity dynamics in the resting state. *Cereb. Cortex* 24, 663–676. <https://doi.org/10.1093/cercor/bhs352>.
- Andersen, N., 1984. The Scale for the Assessment of Positive Symptoms (SAPS).
- Andersen, N.C., 1989. The scale for the assessment of negative symptoms (SANS): conceptual and theoretical foundations. *Br. J. Psychiatry Suppl.* 49–58.
- Ashok, A.H., Marques, T.R., Jauhar, S., Nour, M.M., Goodwin, G.M., Young, A.H., Howes, O.D., 2017. The dopamine hypothesis of bipolar affective disorder: the state of the art and implications for treatment. *Mol. Psychiatry*. <https://doi.org/10.1038/mp.2017.16>.
- Bharath, R.D., Panda, R., Saini, J., Sriganesh, K., Rao, G.S.U., 2017. Dynamic local connectivity uncovers altered brain synchrony during propofol sedation. *Sci. Rep.* 7 <https://doi.org/10.1038/s41598-017-08135-2>.
- Bhinge, S., Long, Q., Calhoun, V.D., Adali, T., 2019. Spatial dynamic functional connectivity analysis identifies distinctive biomarkers in schizophrenia. *Front. Neurosci.* 13 <https://doi.org/10.3389/fnins.2019.01006>.
- Biswal, B.B., van Kylen, J., Hyde, J.S., 1997. Simultaneous assessment of flow and BOLD signals in resting-state functional connectivity maps. *NMR Biomed.* 10, 165–170. [https://doi.org/10.1002/\(SICI\)1099-1492\(199706/08\)10:4/5<165::AID-NBM454>3.0.CO;2-7](https://doi.org/10.1002/(SICI)1099-1492(199706/08)10:4/5<165::AID-NBM454>3.0.CO;2-7).
- Braun, U., Schäfer, A., Bassett, D.S., Rausch, F., Schweiger, J.L., Bilek, E., Erk, S., Romanczuk-Seiferth, N., Grimm, O., Geiger, L.S., Haddad, L., Otto, K., Mohnke, S., Heinz, A., Zink, M., Walter, H., Schwarz, E., Meyer-Lindenberg, A., Tost, H., 2016. Dynamic brain network reconfiguration as a potential schizophrenia genetic risk mechanism modulated by NMDA receptor function. *Proc. Natl. Acad. Sci. U. S. A.* 113, 12568–12573. <https://doi.org/10.1073/pnas.1608819113>.
- Briend, F., Armstrong, W.P., Kraguljac, N.V., Keilholtz, S.D., Lahti, A.C., 2020. Aberrant static and dynamic functional patterns of frontoparietal control network in antipsychotic-naïve first-episode psychosis subjects. *Hum. Brain Mapp.* 41, 2999–3008. <https://doi.org/10.1002/hbm.24992>.
- Buckner, R.L., Andrews-Hanna, J.R., Schacter, D.L., 2008. The brain's default network: anatomy, function, and relevance to disease. *Ann. N. Y. Acad. Sci.* <https://doi.org/10.1196/annals.1440.011>.
- Calhoun, V.D., Adali, T., Pearson, G.D., Pekar, J.J., 2001. A method for making group inferences from functional MRI data using independent component analysis. *Hum. Brain Mapp.* 14, 140. <https://doi.org/10.1002/HBM.1048>.
- Cattarinussi, G., Kubera, K.M., Hirjak, D., Wolf, R.C., Sambataro, F., 2022. Neural correlates of the risk for schizophrenia and bipolar disorder: a meta-analysis of structural and functional neuroimaging studies. *Biol. Psychiatry*. <https://doi.org/10.1016/j.biopsych.2022.02.960>.
- Chen, C.H., Suckling, J., Lennox, B.R., Ooi, C., Bullmore, E.T., 2011. A quantitative meta-analysis of fMRI studies in bipolar disorder. *Bipolar Disord.* <https://doi.org/10.1111/j.1399-5618.2011.00893.x>.
- Chen, G., Chen, P., Gong, J.Y., Jia, Y., Zhong, S., Chen, F., Wang, J., Luo, Z., Qi, Z., Huang, L., Wang, Y., 2022. Shared and specific patterns of dynamic functional connectivity variability of striato-cortical circuitry in unmedicated bipolar and major depressive disorders. *Psychol. Med.* 52, 747–756. <https://doi.org/10.1017/S0033291720002378>.
- Choi, Y.K., Gardner, M.P., Tarazi, F.I., 2009. Effects of risperidone on glutamate receptor subtypes in developing rat brain. *Eur. Neuropsychopharmacol.* 19, 77–84. <https://doi.org/10.1016/j.euroneuro.2008.08.010>.
- Dai, Z., Chen, Y., Li, J., Fam, J., Bezerianos, A., Sun, Y., 2016. Temporal efficiency evaluation and small-worldness characterization in temporal networks. *Sci. Rep.* 6, 1–12. <https://doi.org/10.1038/srep34291>.
- Damaraju, E., Allen, E.A., Belger, A., Ford, J.M., McEwen, S., Mathalon, D.H., Mueller, B.A., Pearson, G.D., Potkin, S.G., Preda, A., Turner, J.A., Vaidya, J.G., van Erp, T.G., Calhoun, V.D., 2014. Dynamic functional connectivity analysis reveals transient states of dysconnectivity in schizophrenia. *Neuroimage Clin.* 5, 298–308. <https://doi.org/10.1016/j.nicl.2014.07.003>.
- Das, T.K., Kumar, J., Francis, S., Liddle, P.F., Palaniyappan, L., 2020. Parietal lobe and disorganisation syndrome in schizophrenia and psychotic bipolar disorder: A bimodal connectivity study. *Psychiatry Res. Neuroimaging* 303. <https://doi.org/10.1016/j.pscychres.2020.111139>.
- Delfino, R.S., Surjan, J., Bandeira, I.D., Brazilliano, L., Correia-Melo, F.S., Del-Porto, J.A., Quarantini, L.C., Lacerda, A.L.T., 2020. NMDA antagonists and their role in the Management of Bipolar Disorder: a review. *Curr. Behav. Neurosci. Rep.* <https://doi.org/10.1007/s40473-020-00201-w>.
- Deng, Y., Liu, K., Cheng, D., Zhang, J., Chen, H., Chen, B., Li, Y., Wang, W., Kong, Y., Wen, G., 2019. Ventral and dorsal visual pathways exhibit abnormalities of static and dynamic connectivities, respectively, in patients with schizophrenia. *Schizophr. Res.* 206, 103–110. <https://doi.org/10.1016/j.schres.2018.12.005>.
- Deng, Y., Han, S., Cheng, D., Li, H., Zhang, B., Kong, Y., Lin, Y., Li, Y., Wen, G., Liu, K., 2021. Simultaneously decreased temporal variability and enhanced variability-strength coupling of emotional network connectivities are related to positive symptoms in patients with schizophrenia. *Brain Imag. Behav.* 15, 76–84. <https://doi.org/10.1007/s11682-019-00234-0>.
- Dong, D., Wang, Y., Chang, X., Luo, C., Yao, D., 2018. Dysfunction of large-scale brain networks in schizophrenia: a meta-analysis of resting-State functional connectivity. *Schizophr. Bull.* 44, 168–181. <https://doi.org/10.1093/SCHBUL/SBX034>.
- Dong, D., Duan, M., Wang, Y., Zhang, X., Jia, X., Li, Y., Xin, F., Yao, D., Luo, C., 2019. Reconfiguration of dynamic functional connectivity in sensory and perceptual system in schizophrenia. *Cereb. Cortex* 29, 3577–3589. <https://doi.org/10.1093/cercor/bhy232>.
- Du, Y., Pearson, G.D., Yu, Q., He, H., Lin, D., Sui, J., Wu, L., Calhoun, V.D., 2016. Interaction among subsystems within default mode network diminished in schizophrenia patients: a dynamic connectivity approach. *Schizophr. Res.* 170, 55–65. <https://doi.org/10.1016/j.schres.2015.11.021>.
- Du, Y., Pearson, G.D., Lin, D., Sui, J., Chen, J., Salman, M., Tamminga, C.A., Ivleva, E.I., Sweeney, J.A., Keshavan, M.S., Clementz, B.A., Bustillo, J., Calhoun, V.D., 2017. Identifying dynamic functional connectivity markers using GIG-ICA: application to schizophrenia, schizoaffective disorder, and psychotic bipolar disorder. *Hum. Brain Mapp.* 38, 2683–2708. <https://doi.org/10.1002/hbm.23553>.
- Du, Y., Fryer, S.L., Fu, Z., Lin, D., Sui, J., Chen, J., Damaraju, E., Mennigen, E., Stuart, B., Loewy, R.L., Mathalon, D.H., Calhoun, V.D., 2018. Dynamic functional connectivity impairments in early schizophrenia and clinical high-risk for psychosis. *Neuroimage* 180, 632–645. <https://doi.org/10.1016/j.neuroimage.2017.10.022>.
- Du, Y., Hao, H., Wang, S., Pearson, G.D., Calhoun, V.D., 2020. Identifying commonality and specificity across psychosis sub-groups via classification based on features from dynamic connectivity analysis. *Neuroimage Clin.* 27 <https://doi.org/10.1016/j.nicl.2020.102284>.
- Du, M., Zhang, L., Li, L., Ji, E., Han, X., Huang, G., Liang, Z., Shi, L., Yang, H., Zhang, Z., 2021a. Abnormal transitions of dynamic functional connectivity states in bipolar disorder: a whole-brain resting-state fMRI study. *J. Affect. Disord.* 289, 7–15. <https://doi.org/10.1016/j.jad.2021.04.005>.
- Du, Y., He, X., Calhoun, V.D., 2021b. A new semi-supervised non-negative matrix factorization method for brain dynamic functional connectivity analysis. In: *Proceedings - International Symposium on Biomedical Imaging. IEEE Computer Society*, pp. 1591–1594. <https://doi.org/10.1109/ISBI48211.2021.9433988>.
- Duan, X., Hu, M., Huang, X., Su, C., Zong, X., Dong, X., He, C., Xiao, J., Li, H., Tang, J., Chen, X., Chen, H., 2020. Effect of risperidone monotherapy on dynamic functional connectivity of insular subdivisions in treatment-naïve, first-episode schizophrenia. *Schizophr. Bull.* 46, 650–660. <https://doi.org/10.1093/schbul/sbz087>.
- Ellard, K.K., Gosai, A.K., Felicione, J.M., Peters, A.T., Shea, C.V., Sylvia, L.G., Nierenberg, A.A., Widge, A.S., Dougherty, D.D., Deckersbach, T., 2019. Deficits in frontoparietal activation and anterior insula functional connectivity during regulation of cognitive-affective interference in bipolar disorder. *Bipolar Disord.* 21, 244–258. <https://doi.org/10.1111/bdi.12709>.
- Espinoza, F.A., Vergara, V.M., Damaraju, E., Henke, K.G., Faghiri, A., Turner, J.A., Belger, A.A., Ford, J.M., McEwen, S.C., Mathalon, D.H., Mueller, B.A., Potkin, S.G., Preda, A., Vaidya, J.G., van Erp, T.G.M., Calhoun, V.D., 2019. Characterizing whole brain temporal variation of functional connectivity via zero and first order derivatives of sliding window correlations. *Front. Neurosci.* 13 <https://doi.org/10.3389/fnins.2019.00634>.
- Faghiri, A., Iraj, A., Damaraju, E., Belger, A., Ford, J., Mathalon, D., McEwen, S., Mueller, B., Pearson, G., Preda, A., Turner, J., Vaidya, J.G., van Erp, T., Calhoun, V.D., 2020. Weighted average of shared trajectory: a new estimator for dynamic functional connectivity efficiently estimates both rapid and slow changes over time. *J. Neurosci. Methods* 334. <https://doi.org/10.1016/j.jneumeth.2020.108600>.
- Faghiri, A., Iraj, A., Damaraju, E., Turner, J., Calhoun, V.D., 2021. A unified approach for characterizing static/dynamic connectivity frequency profiles using filter banks. *Network Neurosci.* 5, 56–82. <https://doi.org/10.1162/netn.a.00155>.
- Fateh, A.A., Cui, Q., Duan, X., Yang, Y., Chen, Y., Li, D., He, Z., Chen, H., 2020. Disrupted dynamic functional connectivity in right amygdalar subregions differentiates bipolar disorder from major depressive disorder. *Psychiatry Res. Neuroimaging* 304. <https://doi.org/10.1016/j.pscychres.2020.111149>.
- Fountoulakis, Konstantinos N., 2012. The possible involvement of NMDA glutamate receptor in the Etiopathogenesis of bipolar disorder. *Curr. Pharm. Des.* 18, 1605–1608. <https://doi.org/10.2174/138161212799958585>.
- Fransson, P., 2005. Spontaneous low-frequency BOLD signal fluctuations: an fMRI investigation of the resting-state default mode of brain function hypothesis. *Hum. Brain Mapp.* 26, 15–29. <https://doi.org/10.1002/hbm.20113>.
- Fu, Z., Tu, Y., Di, X., Du, Y., Pearson, G.D., Turner, J.A., Biswal, B.B., Zhang, Z., Calhoun, V.D., 2018. Characterizing dynamic amplitude of low-frequency fluctuation and its relationship with dynamic functional connectivity: an application to schizophrenia. *Neuroimage*. <https://doi.org/10.1016/j.neuroimage.2017.09.035>.

- Friston, K.J., Frith, C.D., 1995. Schizophrenia: a disconnection syndrome? *Clin. Neurosci.* 3 (2), 89–97.
- Fu, Z., Sui, J., Turner, J.A., Du, Y., Assaf, M., Pearlson, G.D., Calhoun, V.D., 2021. Dynamic functional network reconfiguration underlying the pathophysiology of schizophrenia and autism spectrum disorder. *Hum. Brain Mapp.* 42, 80–94. <https://doi.org/10.1002/hbm.25205>.
- Garcia, J.O., Ashourvan, A., Muldoon, S., Vettel, J.M., Bassett, D.S., 2018. Applications of community detection techniques to brain graphs: algorithmic considerations and implications for neural function. *Proc. IEEE*. <https://doi.org/10.1109/JPROC.2017.2786710>.
- Geng, H., Xu, P., Sommer, I.E., Luo, Y.J., Aleman, A., Ćurčić-Blake, B., 2020. Abnormal dynamic resting-state brain network organization in auditory verbal hallucination. *Brain Struct. Funct.* 225, 2315–2330. <https://doi.org/10.1007/s00429-020-02119-1>.
- Gifford, G., Crossley, N., Kempton, M.J., Morgan, S., Dazzan, P., Young, J., McGuire, P., 2020. Resting state fMRI based multimodal network configuration in patients with schizophrenia. *Neuroimage Clin.* 25. <https://doi.org/10.1016/j.nicl.2020.102169>.
- Gong, J., Wang, Junjing, Chen, P., Qi, Z., Luo, Z., Wang, Jurong, Huang, L., Wang, Y., 2021. Large-scale network abnormality in bipolar disorder: a multimodal meta-analysis of resting-state functional and structural magnetic resonance imaging studies. *J. Affect. Disord.* 292, 9–20. <https://doi.org/10.1016/j.jad.2021.05.052>.
- Guo, S., Zhao, W., Tao, H., Liu, Z., Palaniyappan, L., 2018. The instability of functional connectivity in patients with schizophrenia and their siblings: a dynamic connectivity study. *Schizophr. Res.* 195, 183–189. <https://doi.org/10.1016/j.schres.2017.09.035>.
- Hamilton, M., 1959. The assessment of anxiety states by rating. *Br. J. Med. Psychol.* 32, 50–55. <https://doi.org/10.1111/J.2044-8341.1959.TB00467.X>.
- Hamilton, M., 1960. A rating scale for depression. *J. Neurol. Neurosurg. Psychiatry* 23, 56–62. <https://doi.org/10.1136/JNPP.23.1.56>.
- Han, S., Cui, Q., Wang, X., Li, L., Li, D., He, Z., Guo, X., Fan, Y.S., Guo, J., Sheng, W., Lu, F., Chen, H., 2020. Resting state functional network switching rate is differently altered in bipolar disorder and major depressive disorder. *Hum. Brain Mapp.* 41, 3295–3304. <https://doi.org/10.1002/hbm.25017>.
- Hare, Stephanie M., Ford, J.M., Mathalon, D.H., Damaraju, E., Bustillo, J., Belger, A., Lee, H.J., Mueller, B.A., Lim, K.O., Brown, G.G., Preda, A., van Erp, T.G.M., Potkin, S.G., Calhoun, V.D., Turner, J.A., 2019a. Salience–default mode functional network connectivity linked to positive and negative symptoms of Schizophrenia. *Schizophr. Bull.* 45, 892–901. <https://doi.org/10.1093/schbul/sby112>.
- Hare, Stephanie M., Ford, J.M., Mathalon, D.H., Damaraju, E., Bustillo, J., Belger, A., Lee, H.J., Mueller, B.A., Lim, K.O., Brown, G.G., Preda, A., van Erp, T.G.M., Potkin, S.G., Calhoun, V.D., Turner, J.A., 2019b. Salience–default mode functional network connectivity linked to positive and negative symptoms of Schizophrenia. *Schizophr. Bull.* 45, 892. <https://doi.org/10.1093/SCHBUL/SBY112>.
- Harlalka, V., Bapi, R.S., Vinod, P.K., Roy, D., 2019. Atypical flexibility in dynamic functional connectivity quantifies the severity in autism spectrum disorder. *Front. Hum. Neurosci.* 13. <https://doi.org/10.3389/fnhum.2019.00006>.
- Harvey, P.O., Lee, J., Cohen, M.S., Engel, S.A., Glahn, D.C., Nuechterlein, K.H., Wynn, J. K., Green, M.F., 2011. Altered dynamic coupling of lateral occipital complex during visual perception in schizophrenia. *Neuroimage* 55, 1219–1226. <https://doi.org/10.1016/j.neuroimage.2010.12.045>.
- He, H., Luo, C., Luo, Y., Duan, M., Yi, Q., Biswal, B.B., Yao, D., 2019. Reduction in gray matter of cerebellum in schizophrenia and its influence on static and dynamic connectivity. *Hum. Brain Mapp.* 40, 517–528. <https://doi.org/10.1002/hbm.24391>.
- He, H., Luo, C., He, C., He, M., Du, J., Biswal, B.B., Yao, D., Yao, G., Duan, M., 2021. Altered spatial organization of dynamic functional network associates with deficient sensory and perceptual network in Schizophrenia. *Front Psychiatry* 12. <https://doi.org/10.3389/fpsy.2021.687580>.
- Hutchison, R.M., Womelsdorf, T., Allen, E.A., Bandettini, P.A., Calhoun, V.D., Corbetta, M., Della Penna, S., Duyn, J.H., Glover, G.H., Gonzalez-Castillo, J., Handwerker, D.A., Keilholz, S., Kiviniemi, V., Leopold, D.A., de Pasquale, F., Sporns, O., Walter, M., Chang, C., 2013. Dynamic functional connectivity: promise, issues, and interpretations. *Neuroimage* 80, 360–378. <https://doi.org/10.1016/j.neuroimage.2013.05.079>.
- Jia, Y., Gu, H., 2019. Identifying nonlinear dynamics of brain functional networks of patients with schizophrenia by sample entropy. *Nonlinear Dyn.* <https://doi.org/10.1007/s11071-019-04924-8>.
- Jia, Y., Gu, H., Luo, Q., 2017. Sample entropy reveals an age-related reduction in the complexity of dynamic brain. *Sci. Rep.* 7. <https://doi.org/10.1038/s41598-017-08565-y>.
- Jimenez, A.M., Riedel, P., Lee, J., Reavis, E.A., Green, M.F., 2019. Linking resting-state networks and social cognition in schizophrenia and bipolar disorder. *Hum. Brain Mapp.* 40, 4703. <https://doi.org/10.1002/hbm.24731>.
- Kaufmann, T., Skåtun, K.C., Alnæs, D., Doan, N.T., Duff, E.P., Tønnesen, S., Roussos, E., Ueland, T., Aminoff, S.R., Lagerberg, T.V., Agartz, I., Melle, I.S., Smith, S.M., Andreassen, O.A., Westlye, L.T., 2015. Disintegration of sensorimotor brain networks in schizophrenia. *Schizophr. Bull.* 41, 1326–1335. <https://doi.org/10.1093/schbul/sbv060>.
- Kay, S.R., Fiszbein, A., Opler, L.A., 1987. The positive and negative syndrome scale (PANSS) for schizophrenia. *Schizophr. Bull.* 13, 261–276. <https://doi.org/10.1093/SCHBUL/13.2.261>.
- Kubera, K.M., Rashidi, M., Schmitgen, M.M., Barth, A., Hirjak, D., Sambataro, F., Calhoun, V.D., Wolf, R.C., 2019. Structure/function interrelationships in patients with schizophrenia who have persistent auditory verbal hallucinations: a multimodal MRI study using parallel ICA. *Prog. Neuro-Psychopharmacol. Biol. Psychiatry* 93, 114–121. <https://doi.org/10.1016/j.pnpbp.2019.03.007>.
- Lee, M.H., Smyser, C.D., Shimony, J.S., 2013a. Resting-State fMRI: a review of methods and clinical applications. *AJNR Am. J. Neuroradiol.* 34, 1866. <https://doi.org/10.3174/AJNR.A3263>.
- Lee, S.H., Ripke, S., Neale, B.M., Faraone, S.V., Purcell, S.M., Perlis, R.H., Mowry, B.J., Thapar, A., Goddard, M.E., Witte, J.S., Absher, D., Agartz, I., Akil, H., Amin, F., Andreassen, O.A., Anjorin, A., Anney, R., Antilla, V., Arking, D.E., Asherson, P., Azevedo, M.H., Backlund, L., Badner, J.A., Bailey, A.J., Banaschewski, T., Barchas, J. D., Barnes, M.R., Barrett, T.B., Bass, N., Battaglia, A., Bauer, M., Bayés, M., Bellivier, F., Bergen, S.E., Berrettini, W., Betancur, C., Bettecken, T., Biederman, J., Binder, E.B., Black, D.W., Blackwood, D.H.R., Bloss, C.S., Boehnke, M., Boomsma, D. I., Breen, G., Breuer, R., Bruggeman, R., Cormican, P., Buccola, N.G., Buitema, J.K., Bunnay, W.E., Buxbaum, J.D., Byerley, W.F., Byrne, E.M., Caesar, S., Cahn, W., Cantor, R.M., Casas, M., Chakravarti, A., Chambert, K., Choudhury, K., Cichon, S., Cloninger, C.R., Collier, D.A., Cook, E.H., Coon, H., Cormand, B., Corvin, A., Coryell, W.H., Craig, D.W., Craig, I.W., Crosbie, J., Cuccaro, M.L., Curtis, D., Czamara, D., Datta, S., Dawson, G., Day, R., de Geus, E.J., Degenhardt, F., Djurovic, S., Donohoe, G.J., Doyle, A.E., Duan, J., Dudbridge, F., Duketis, E., Ebstein, R.P., Edenberg, H.J., Elia, J., Ennis, S., Etain, B., Fanous, A., Farmer, A.E., Faraone, S.V., Flickinger, M., Fombonne, E., Foroud, T., Frank, J., Franke, B., Fraser, C., Freedman, R., Freimer, N.B., Freitag, C.M., Friedl, M., Frisén, L., Gallagher, L., Gejman, P.v., Georgieva, L., Gershon, E.S., Geschwind, D.H., Giegling, I., Gill, M., Gordon, S.D., Gordon-Smith, K., Green, E.K., Greenwood, T.A., Grice, D.E., Gross, M., Grozeva, D., Guan, W., Gurling, H., de Haan, L., Haines, J.L., Hakonarson, H., Hallmayer, J., Hamilton, S.P., Hamshere, M.L., Hansen, T.F., Hartmann, A.M., Hautzinger, M., Heath, A.C., Henders, A.K., Herms, S., Hickie, I.B., Hipolito, M., Hoefels, S., Holmans, P.A., Holsboer, F., Hoogendijk, W.J., Hottenga, J. J., Hultman, C.M., Hus, V., Ingason, A., Ising, M., Jamain, S., Jones, E.G., Jones, I., Jones, L., Tzeng, J.Y., Kähler, A.K., Kahn, R.S., Kandaswamy, R., Keller, M.C., Kennedy, J.L., Kenny, E., Kent, L., Kim, Y., Kirov, G.K., Klauk, S.M., Klei, L., Knowles, J.A., Kohli, M.A., Koller, D.L., Konte, B., Korszun, A., Krabbendam, L., Krasucki, R., Kuntsi, J., Kwan, P., Landén, M., Långström, N., Lathrop, M., Lawrence, J., Lawson, W.B., Leboyer, M., Ledbetter, D.H., Lee, P.H., Lencz, T., Lesch, K.P., Levinson, D.F., Lewis, C.M., Li, J., Lichtenstein, P., Lieberman, J.A., Lin, D.Y., Linszen, D.H., Liu, C., Lohoff, F.W., Loo, S.K., Lord, C., Lowe, J.K., Lucae, S., Macintyre, D.J., Madden, P.A.F., Maestrini, E., Magnusson, P.K.E., Mahon, P.B., Maier, W., Malhotra, A.K., Mane, S.M., Martin, C.L., Martin, N.G., Mattheisen, M., Matthews, K., Mattingdal, M., Mccarroll, S.A., McGhee, K.A., McGough, J.J., McGrath, P.J., McGuffin, P., Mcinnis, M.G., McIntosh, A., Mckinney, R., Mclean, A.W., McMahon, F.J., McMahon, W.M., Mcquillin, A., Meeiros, H., Mcland, S.E., Meier, S., Melle, I., Meng, F., Meyer, J., Middeldorp, C. M., Middleton, L., Milanova, V., Miranda, A., Monaco, A.P., Montgomery, G.W., Moran, J.L., Moreno-De-Luca, D., Morken, G., Morris, D.W., Morrow, E.M., Moskvina, V., Muglia, P., Mühleisen, T.W., Muir, W.J., Müller-Myhsok, B., Murtha, M., Myers, R.M., Myin-Germeys, I., Neale, M.C., Nelson, S.F., Nievergelt, C. M., Nikolov, I., Ningaonkar, V., Nolte, W.A., Nöthen, M.M., Nurnberger, J.I., Nwulia, E.A., Nyholt, D.R., O'dushlaine, C., Oades, R.D., Olincy, A., Oliveira, G., Olsen, L., Ophoff, R.A., Osby, U., Owen, M.J., Palotie, A., Parr, J.R., Paterson, A.D., Pato, C.N., Pato, M.T., Penninx, B.W., Pergadia, M.L., Pericak-Vance, M.A., Pickard, B.S., Pimm, J., Piven, J., Posthuma, D., Potash, J.B., Poustka, F., Propping, P., Puri, V., Quedest, D.J., Quinn, E.M., Ramos-Quiroga, J.A., Rasmussen, H.B., Raychaudhuri, S., Rehnström, K., Reif, A., Ribasés, M., Rice, J.P., Rietschel, M., Roeder, K., Roeyers, H., Rossin, L., Rothenberger, A., Rouleau, G., Ruderfer, D., Rujescu, D., Sanders, A.R., Sanders, S.J., Santangelo, S.L., Sergeant, J. A., Schachar, R., Schalling, M., Schatzberg, A.F., Schefner, W.A., Schellenberg, G.D., Scherer, S.W., Schork, N.J., Schulze, T.G., Schumacher, J., Schwarz, M., Scolnick, E., Scott, L.J., Shi, J., Shilling, P.D., Shyn, S.I., Silverman, J.M., Slager, S.L., Smalley, S. L., Smit, J.H., Smith, E.N., Sonuga-Barke, E.J.S., St. Clair, D., State, M., Steffens, M., Steinhausen, H.C., Strauss, J.S., Strohmaier, J., Stroup, T.S., Sutcliffe, J.S., Szatmari, P., Szelinger, S., Thirumalai, S., Thompson, R.C., Todorov, A.A., Tozzi, F., Treutlein, J., Uhr, M., van den Oord, E.J.C.G., van Grootheest, G., van Os, J., Vicente, A.M., Vieland, V.J., Vincent, J.B., Visscher, P.M., Walsh, C.A., Wassink, T. H., Watson, S.J., Weissman, M.M., Werge, T., Wienker, T.F., Wijsman, E.M., Willemssen, G., Williams, N., Willsey, A.J., Witt, S.H., Xu, W., Young, A.H., Yu, T.W., Zammit, S., Zandi, P.P., Zhang, P., Zitman, F.G., Zöllner, S., Devlin, B., Kelsoe, J.R., Sklar, P., Daly, M.J., O'donovan, M.C., Craddock, N., Sullivan, P.F., Smoller, J.W., Kendler, K.S., Wray, N.R., 2013b. Genetic relationship between five psychiatric disorders estimated from genome-wide SNPs. *Nat. Genet.* 45, 984–994. <https://doi.org/10.1038/NG.2711>.
- Lee, R.S.C., Hermens, D.F., Naismith, S.L., Lagopoulos, J., Jones, A., Scott, J., Chitty, K. M., White, D., Robillard, R., Scott, E.M., Hickie, I.B., 2015. Neuropsychological and functional outcomes in recent-onset major depression, bipolar disorder and schizophrenia-spectrum disorders: a longitudinal cohort study. *Transl. Psychiatry* 5, e555. <https://doi.org/10.1038/TP.2015.50>.
- Lee, W.H., Doucet, G.E., Leib, E., Frangou, S., 2018. Resting-state network connectivity and metastability predict clinical symptoms in schizophrenia. *Schizophr. Res.* 201, 208–216. <https://doi.org/10.1016/j.schres.2018.04.029>.
- Leroy, A., Amad, A., D'hondt, F., Pins, D., Jaafari, N., Thomas, P., Jardri, R., 2020. Reward anticipation in schizophrenia: a coordinate-based meta-analysis. *Schizophr. Res.* 218, 2–6. <https://doi.org/10.1016/J.SCHRES.2019.12.041>.
- Li, C.T., Tu, P.C., Hsieh, J.C., Lee, H.C., Bai, Y.M., Tsai, C.F., Wang, S.J., Hsu, J.W., Huang, K.L., Hsong, C.J., Su, T.P., 2015. Functional dysconnection in the prefrontal-amygdala circuitry in unaffected siblings of patients with bipolar I disorder. *Bipolar Disord.* 17, 626–635. <https://doi.org/10.1111/BDI.12321>.
- Li, K., Sweeney, J.A., Hu, X.P., 2020. Context-dependent dynamic functional connectivity alteration of lateral occipital cortex in schizophrenia. *Schizophr. Res.* 220, 201–209. <https://doi.org/10.1016/j.schres.2020.03.020>.

- Li, C., Dong, M., Womer, F.Y., Han, S., Yin, Y., Jiang, X., Wei, Y., Duan, J., Feng, R., Zhang, L., Zhang, X., Wang, F., Tang, Y., Xu, K., 2021. Transdiagnostic time-varying dysconnectivity across major psychiatric disorders. *Hum. Brain Mapp.* 42, 1182–1196. <https://doi.org/10.1002/hbm.25285>.
- Liang, Y., Jiang, X., Zhu, W., Shen, Y., Xue, F., Li, Y., Chen, Z., 2020. Disturbances of dynamic function in patients with bipolar disorder I and its relationship with executive-function deficit. *Front Psychiatry* 11. <https://doi.org/10.3389/fpsy.2020.537981>.
- Liddle, P.F., Ngan, E.T.C., Duffield, G., Kho, K., Warren, A.J., 2002. Signs and symptoms of psychotic illness (SSPI): a rating scale. *Br. J. Psychiatry* 180, 45–50. <https://doi.org/10.1192/BJP.180.1.45>.
- Liu, M., Wang, Yuchen, Zhang, A., Yang, C., Liu, P., Wang, J., Zhang, K., Wang, Yanfang, Sun, N., 2021. Altered dynamic functional connectivity across mood states in bipolar disorder. *Brain Res.* 1750 <https://doi.org/10.1016/j.brainres.2020.147143>.
- Lloyd, S.P., 1982. Least squares quantization in PCM. *IEEE Trans. Inf. Theory* 28, 129–137. <https://doi.org/10.1109/TIT.1982.1056489>.
- Long, Y., Liu, Z., Chan, C.K.Y., Wu, G., Xue, Z., Pan, Y., Chen, X., Huang, X., Li, D., Pu, W., 2020. Altered temporal variability of local and large-scale resting-State brain functional connectivity patterns in schizophrenia and bipolar disorder. *Front Psychiatry* 11. <https://doi.org/10.3389/fpsy.2020.00422>.
- Long, Q., Bhinge, S., Calhoun, V.D., Adali, T., 2021. Graph-theoretical analysis identifies transient spatial states of resting-state dynamic functional network connectivity and reveals dysconnectivity in schizophrenia. *J. Neurosci. Methods* 350. <https://doi.org/10.1016/j.jneumeth.2020.109039>.
- Lottman, K.K., Kraguljac, N.V., White, D.M., Morgan, C.J., Calhoun, V.D., Butt, A., Lahti, A.C., 2017. Risperidone effects on brain dynamic connectivity-A prospective resting-state fMRI study in schizophrenia. *Front Psychiatry* 8. <https://doi.org/10.3389/fpsy.2017.00014>.
- Luo, X., Chen, G., Jia, Y., Gong, J.Y., Qiu, S., Zhong, S., Zhao, L., Chen, F., Lai, S., Qi, Z., Huang, L., Wang, Y., 2018. Disrupted cerebellar connectivity with the central executive network and the default-mode network in unmedicated bipolar II disorder. *Front Psychiatry* 9, 705. <https://doi.org/10.3389/fpsy.2018.00705>.
- Luo, Y., He, H., Duan, M., Huang, H., Hu, Z., Wang, H., Yao, G., Yao, D., Li, J., Luo, C., 2020. Dynamic functional connectivity strength within different frequency-band in schizophrenia. *Front Psychiatry* 10. <https://doi.org/10.3389/fpsy.2019.00995>.
- Luo, Z., Chen, G., Jia, Y., Zhong, S., Gong, J., Chen, F., Wang, J., Qi, Z., Liu, X., Huang, L., Wang, Y., 2021. Shared and specific dynamics of brain segregation and integration in bipolar disorder and major depressive disorder: a resting-state functional magnetic resonance imaging study. *J. Affect. Disord.* 280, 279–286. <https://doi.org/10.1016/j.jad.2020.11.012>.
- Manoliu, A., Riedl, V., Zherdin, A., Mühlau, M., Schwerthöffer, D., Scherr, M., Peters, H., Zimmer, C., Förstl, H., Bäuml, J., Wohlschläger, A.M., Sorg, C., 2014. Aberrant dependence of default mode/central executive network interactions on anterior insular salience network activity in schizophrenia. *Schizophr. Bull.* 40, 428–437. <https://doi.org/10.1093/SCHBUL/SBT037>.
- Mennigen, E., Fryer, S.L., Rashid, B., Damaraju, E., Du, Y., Loewy, R.L., Stuart, B.K., Calhoun, V.D., Mathalon, D.H., 2019. Transient patterns of functional dysconnectivity in clinical high risk and early illness schizophrenia individuals compared with healthy controls. *Brain Connect* 9, 60–76. <https://doi.org/10.1089/brain.2018.0579>.
- Menon, V., 2011. Large-scale brain networks and psychopathology: a unifying triple network model. *Trends Cogn. Sci.* 15, 483–506. <https://doi.org/10.1016/j.tics.2011.08.003>.
- Menon, B., 2019. Towards a new model of understanding – the triple network, psychopathology and the structure of the mind. *Med. Hypotheses* 133. <https://doi.org/10.1016/j.mehy.2019.109385>.
- Merritt, K., McGuire, P., Egerton, A., 2013. Relationship between glutamate dysfunction and symptoms and cognitive function in psychosis. *Front Psychiatry* 4, 151. <https://doi.org/10.3389/fpsy.2013.00151>.
- Miller, T.J., Mcqlashan, T.H., Rosen, J.L., Cadenhead, K., Ventura, J., Mcfarlane, W., Perkins, D.O., Pearson, Q.D., Woods, S.W., 2003. Prodrimal Assessment with the Structured Interview for Prodrimal Syndromes and the Scale of Prodrimal Symptoms: Predictive Validity, Interrater Reliability, and Training to Reliability.
- Miller, R.L., Vergara, V.M., Keator, D.B., Calhoun, V.D., 2016a. A method for intertemporal functional-domain connectivity analysis: application to schizophrenia reveals distorted directional information flow. *IEEE Trans. Biomed. Eng.* 63, 2525–2539. <https://doi.org/10.1109/TBME.2016.2600637>.
- Miller, R.L., Vergara, V.M., Keator, D.B., Calhoun, V.D., 2016b. A method for intertemporal functional-domain connectivity analysis: application to schizophrenia reveals distorted directional information flow. *IEEE Trans. Biomed. Eng.* 63, 2525–2539. <https://doi.org/10.1109/TBME.2016.2600637>.
- Miller, R.L., Yaesoubi, M., Turner, J.A., Mathalon, D., Preda, A., Pearson, G., Adali, T., Calhoun, V.D., 2016c. Higher dimensional meta-state analysis reveals reduced resting fMRI connectivity dynamism in schizophrenia patients. *PLoS One* 11. <https://doi.org/10.1371/journal.pone.0149849>.
- Minzenberg, M.J., Laird, A.R., Thelen, S., Carter, C.S., Glahn, D.C., 2009. Meta-analysis of 41 functional neuroimaging studies of executive function in schizophrenia. *Arch. Gen. Psychiatry* 66, 811–822. <https://doi.org/10.1001/ARCHGENPSYCHIATRY.2009.91>.
- Miola, A., Cattarinussi, G., Antiga, G., Caiolo, S., Solmi, M., Sambataro, F., 2022. Difficulties in emotion regulation in bipolar disorder: a systematic review and meta-analysis. *J. Affect. Disord.* 302, 352–360. <https://doi.org/10.1016/j.jad.2022.01.102>.
- Nguyen, T.T., Kovacevic, S., Dev, S.I., Lu, K., Liu, T.T., Eyster, L.T., 2017. Dynamic functional connectivity in bipolar disorder is associated with executive function and processing speed: a preliminary study. *Neuropsychology* 31, 73–83. <https://doi.org/10.1037/neu0000317>.
- Northoff, G., 2015. Is schizophrenia a spatiotemporal disorder of the brain's resting state? *World Psychiatry* 14, 34. <https://doi.org/10.1002/WPS.20177>.
- Northoff, G., 2016. Spatiotemporal psychopathology I: No rest for the brain's resting state activity in depression? Spatiotemporal psychopathology of depressive symptoms. *J. Affect. Disord.* 190, 854–866. <https://doi.org/10.1016/j.jad.2015.05.007>.
- Northoff, G., Duncan, N.W., 2016. How do abnormalities in the brain's spontaneous activity translate into symptoms in schizophrenia? From an overview of resting state activity findings to a proposed spatiotemporal psychopathology. *Prog. Neurobiol.* <https://doi.org/10.1016/j.pneurobio.2016.08.003>.
- Nyatega, C.O., Qiang, L., Adamu, M.J., Younis, A., Kawuwa, H.B., 2021. Altered dynamic functional connectivity of cuneus in schizophrenia patients: a resting-state fmri study. *Appl. Sci. (Switzerl.)* 11. <https://doi.org/10.3390/app11231392>.
- O'Donoghue, S., Holleran, L., Cannon, D.M., McDonald, C., 2017. Anatomical dysconnectivity in bipolar disorder compared with schizophrenia: a selective review of structural network analyses using diffusion MRI. *J. Affect. Disord.* 209, 217–228. <https://doi.org/10.1016/j.jad.2016.11.015>.
- Orlicak, F., Delamillieure, P., Delcroix, N., Naveau, M., Brazo, P., Razafimandimby, A., Dollfus, S., Joliot, M., 2017. Network modeling of resting state connectivity points towards the bottom up theories of schizophrenia. *Psychiatry Res. Neuroimaging* 266, 19–26. <https://doi.org/10.1016/j.pscychresns.2017.04.003>.
- Overall, J.E., Gorham, D.R., 1962. The Brief Psychiatric Rating Scale: Psychological Reports, 10, pp. 799–812. <https://doi.org/10.2466/PRO.1962.10.3.799>.
- Palaniyappan, L., Mallikarjun, P., Joseph, V., White, T.P., Liddle, P.F., 2011. Reality distortion is related to the structure of the salience network in schizophrenia. *Psychol. Med.* 41, 1701–1708. <https://doi.org/10.1017/S0033291710002205>.
- Pang, Y., Chen, Heng, Wang, Y., Long, Z., He, Z., Zhang, H., Liao, W., Cui, Q., Chen, Huafu, 2018. Transdiagnostic and diagnosis-specific dynamic functional connectivity anchored in the right anterior insula in major depressive disorder and bipolar depression. *Prog. Neuro-Psychopharmacol. Biol. Psychiatry* 85, 7–15. <https://doi.org/10.1016/j.pnpbp.2018.03.020>.
- Pang, Y., Zhang, H., Cui, Q., Yang, Q., Lu, F., Chen, Heng, He, Z., Wang, Y., Wang, J., Chen, Huafu, 2020. Combined static and dynamic functional connectivity signatures differentiating bipolar depression from major depressive disorder. *Aust. N. Z. J. Psychiatry* 54, 832–842. <https://doi.org/10.1177/0004867420924089>.
- Phillips, J.R., Hewedi, D.H., Eissa, A.M., Moustafa, A.A., 2015. The cerebellum and psychiatric disorders. *Front. Public Health.* <https://doi.org/10.3389/fpubh.2015.00066>.
- Plis, S.M., Amin, M.F., Chekroud, A., Hjelm, D., Damaraju, E., Lee, H.J., Bustillo, J.R., Cho, K.H., Pearlson, G.D., Calhoun, V.D., 2018. Reading the (functional) writing on the (structural) wall: multimodal fusion of brain structure and function via a deep neural network based translation approach reveals novel impairments in schizophrenia. *Neuroimage* 181, 734–747. <https://doi.org/10.1016/j.neuroimage.2018.07.047>.
- Rabany, L., Brocke, S., Calhoun, V.D., Pittman, B., Corbera, S., Wexler, B.E., Bell, M.D., Pelphey, K., Pearlson, G.D., Assaf, M., 2019. Dynamic functional connectivity in schizophrenia and autism spectrum disorder: convergence, divergence and classification. *Neuroimage Clin.* 24 <https://doi.org/10.1016/j.nicl.2019.101966>.
- Rahaman, M.A., Damaraju, E., Saha, D.K., Calhoun, V.D., Plis, S.M., 2021. Statelets: A novel multi-dimensional state-shape representation of brain functional connectivity dynamics. In: *Proceedings - International Symposium on Biomedical Imaging. IEEE Computer Society*, pp. 1822–1826. <https://doi.org/10.1109/ISBI48211.2021.9433762>.
- Raichle, M.E., 2011. The restless brain. *Brain. Connect* 1, 3. <https://doi.org/10.1089/BRAIN.2011.0019>.
- Ramsay, I.S., 2019. An activation likelihood estimate meta-analysis of thalamocortical dysconnectivity in psychosis. *Biol. Psychiatry Cogn. Neurosci. Neuroimaging* 4, 859–869. <https://doi.org/10.1016/j.bpsc.2019.04.007>.
- Rashid, B., Damaraju, E., Pearlson, G.D., Calhoun, V.D., 2014. Dynamic connectivity states estimated from resting fMRI identify differences among schizophrenia, bipolar disorder, and healthy control subjects. *Front. Hum. Neurosci.* 8 <https://doi.org/10.3389/fnhum.2014.00897>.
- Rey, G., Bolton, T.A.W., Gaviria, J., Piguet, C., Preti, M.G., Favre, S., Aubry, J.M., van de Ville, D., Vuilleumier, P., 2021. Dynamics of amygdala connectivity in bipolar disorders: a longitudinal study across mood states. *Neuropsychopharmacology* 46, 1693–1701. <https://doi.org/10.1038/s41386-021-01038-x>.
- Sakoglu, Ü., Pearlson, G.D., Kiehl, K.A., Wang, Y.M., Michael, A.M., Calhoun, V.D., 2010. A method for evaluating dynamic functional network connectivity and task-modulation: application to schizophrenia. *Magma (New York, N.Y.)* 23 (5–6), 351–366. <https://doi.org/10.1007/S10334-010-0197-8>.
- Salman, M.S., Du, Y., Calhoun, V.D., 2017. Identifying fMRI dynamic connectivity states using affinity propagation clustering method: application to schizophrenia. In: *ICASSP, IEEE International Conference on Acoustics, Speech and Signal Processing - Proceedings*, pp. 904–908. <https://doi.org/10.1109/ICASSP.2017.7952287>.
- Salman, Mustafa S., Vergara, V.M., Damaraju, E., Calhoun, V.D., 2019. Decreased cross-domain mutual information in schizophrenia from dynamic connectivity states. *Front. Neurosci.* 13 <https://doi.org/10.3389/fnins.2019.00873>.
- Sambataro, F., Reed, J.D., Murty, V.P., Das, S., Tan, H.Y., Callicott, J.H., Weinberger, D.R., Mattay, V.S., 2009. Catechol-O-methyltransferase Valine158Methionine polymorphism modulates brain networks underlying working memory across adulthood. *Biol. Psychiatry* 66, 540–548. <https://doi.org/10.1016/j.biopsych.2009.04.014>.
- Sambataro, F., Cattarinussi, G., Lawrence, A., Biaggi, A., Fusté, M., Hazelgrove, K., Mehta, M.A., Pawlby, S., Conroy, S., Seneviratne, G., Craig, M.C., Pariante, C.M.,

- Miele, M., Dazzan, P., 2021a. Altered dynamics of the prefrontal networks are associated with the risk for postpartum psychosis: a functional magnetic resonance imaging study. *Transl. Psychiatry* 11, 1–11. <https://doi.org/10.1038/s41398-021-01351-5>.
- Sambataro, F., Hirjak, D., Fritze, S., Kubera, K.M., Northoff, G., Calhoun, V.D., Meyer-Lindenberg, A., Wolf, R.C., 2021b. Intrinsic neural network dynamics in catatonia. *Hum. Brain Mapp.* 42, 6087–6098. <https://doi.org/10.1002/hbm.25671>.
- Sanfratello, L., Houck, J.M., Calhoun, V.D., 2019. Dynamic functional network connectivity in schizophrenia with magnetoencephalography and functional magnetic resonance imaging: Do different timescales tell a different story? *Brain Connect* 9, 251–262. <https://doi.org/10.1089/brain.2018.0608>.
- Seamans, J.K., Yang, C.R., 2004. The principal features and mechanisms of dopamine modulation in the prefrontal cortex. *Prog. Neurobiol.* <https://doi.org/10.1016/j.pneurobio.2004.05.006>.
- Sendi, M.S.E., Pearson, G.D., Mathalon, D.H., Ford, J.M., Preda, A., van Erp, T.G.M., Calhoun, V.D., 2021a. Multiple overlapping dynamic patterns of the visual sensory network in schizophrenia. *Schizophr. Res.* 228, 103–111. <https://doi.org/10.1016/j.schres.2020.11.055>.
- Sendi, M.S.E., Zendehrouh, E., Ellis, C.A., Liang, Z., Fu, Z., Mathalon, D.H., Ford, J.M., Preda, A., van Erp, T.G.M., Miller, R.L., Pearson, G.D., Turner, J.A., Calhoun, V.D., 2021b. Aberrant dynamic functional connectivity of default mode network in schizophrenia and links to symptom severity. *Front. Neural Circuits* 15. <https://doi.org/10.3389/fncir.2021.649417>.
- Shakil, S., Magnuson, M.E., Keilholz, S.D., Lee, C.H., 2014. Cluster-based analysis for characterizing dynamic functional connectivity. In: 2014 36th Annual International Conference of the IEEE Engineering in Medicine and Biology Society, EMBC 2014. Institute of Electrical and Electronics Engineers Inc., pp. 982–985. <https://doi.org/10.1109/EMBC.2014.6943757>.
- Sheng, D., Pu, W., Linli, Z., Tian, G.L., Guo, S., Fei, Y., 2021. Aberrant global and local dynamic properties in schizophrenia with instantaneous phase method based on Hilbert transform. *Psychol. Med.* <https://doi.org/10.1017/S0033291721003895>.
- Smith, S.M., Fox, P.T., Miller, K.L., Glahn, D.C., Fox, P.M., Mackay, C.E., Filippini, N., Watkins, K.E., Toro, R., Laird, A.R., Beckmann, C.F., 2009. Correspondence of the brain's functional architecture during activation and rest. *Proc. Natl. Acad. Sci.* 106, 13040–13045. <https://doi.org/10.1073/PNAS.0905267106>.
- Smoller, J.W., Kendler, K., Craddock, N., Lee, P.H., Neale, B.M., Nurnberger, J.N., Ripke, S., Santangelo, S., Sullivan, P.S., Neale, B.N., Purcell, S., Anney, R., Buitelaar, J., Faraone, S.F., Hoogendijk, W., Lesch, K.P., Levinson, D.L., Perlis, R.P., Rietschel, M., Riley, B., Sonuga-Barke, E., Schachar, R., Schulze, T.S., Thapar, A., Kendler, K.K., Smoller, J.S., Neale, M., Perlis, R., Bender, P., Cichon, S., Daly, M.D., Kelsoe, J., Lehner, T., Levinson, D., O'Donovan, M., Gejman, P., Sebat, J., Sklar, P., Daly, M., Devlin, B., Sullivan, P., O'Donovan, M., Michael, 2013. Identification of risk loci with shared effects on five major psychiatric disorders: a genome-wide analysis. *Lancet* 381, 1371–1379. [https://doi.org/10.1016/S0140-6736\(12\)62129-1](https://doi.org/10.1016/S0140-6736(12)62129-1).
- Sokunbi, M.O., Staff, R.T., Waiter, G.D., Ahearn, T.S., Fox, H.C., Deary, I.J., Starr, J.M., Whalley, L.J., Murray, A.D., 2011. Inter-individual differences in fMRI entropy measurements in old age. *IEEE Trans. Biomed. Eng.* 58, 3206–3214. <https://doi.org/10.1109/TBME.2011.2164793>.
- Stephan, K.E., Friston, K.J., Frith, C.D., 2009. Dysconnection in schizophrenia: from abnormal synaptic plasticity to failures of self-monitoring. *Schizophr. Bull.* <https://doi.org/10.1093/schbul/sbn176>.
- Stroup, D.F., Berlin, J.A., Morton, S.C., Olkin, I., Williamson, G.D., Rennie, D., Moher, D., Becker, B.J., Sipe, T.A., Thacker, S.B., 2000. Meta-analysis of observational studies in epidemiology: a proposal for reporting. *J. Am. Med. Assoc.* 283, 2008–2012. <https://doi.org/10.1001/jama.283.15.2008>.
- Su, J., Shen, H., Zeng, L.L., Qin, J., Liu, Z., Hu, D., 2016. Heredity characteristics of schizophrenia shown by dynamic functional connectivity analysis of resting-state functional MRI scans of unaffected siblings. *Neuroreport* 27, 843–848. <https://doi.org/10.1097/WNR.0000000000000622>.
- Sun, Y., Collinson, S.L., Suckling, J., Sim, K., 2019. Dynamic reorganization of functional connectivity reveals abnormal temporal efficiency in schizophrenia. *Schizophr. Bull.* 45, 659–669. <https://doi.org/10.1093/schbul/sby077>.
- Sun, F., Zhao, Z., Lan, M., Xu, Y., Huang, M., Xu, D., 2021. Abnormal dynamic functional network connectivity of the mirror neuron system network and the mentalizing network in patients with adolescent-onset, first-episode, drug-naïve schizophrenia. *Neurosci. Res.* 162, 63–70. <https://doi.org/10.1016/j.neures.2020.01.003>.
- Supekar, K., Cai, W., Krishnadas, R., Palaniyappan, L., Menon, V., 2019. Dysregulated brain dynamics in a triple-network saliency model of schizophrenia and its relation to psychosis. *Biol. Psychiatry* 85, 60–69. <https://doi.org/10.1016/j.biopsych.2018.07.020>.
- Tang, Q., Cui, Q., Chen, Y., Deng, J., Sheng, W., Yang, Y., Lu, F., Zeng, Y., Jiang, K., Chen, H., 2022. Shared and distinct changes in local dynamic functional connectivity patterns in major depressive and bipolar depressive disorders. *J. Affect. Disord.* 298, 43–50. <https://doi.org/10.1016/j.jad.2021.10.109>.
- Thoma, R.J., Chaze, C., Lewine, J.D., Calhoun, V.D., Clark, V.P., Bustillo, J., Houck, J., Ford, J., Bigelow, R., Wilhelm, C., Stephen, J.M., Turner, J.A., 2016. Functional MRI evaluation of multiple neural networks underlying auditory verbal hallucinations in schizophrenia spectrum disorders. *Front Psychiatry* 7. <https://doi.org/10.3389/FPSYT.2016.00039>.
- Toschi, N., Duggento, A., Passamonti, L., 2017. Functional connectivity in amygdalar-sensory/(pre)motor networks at rest: new evidence from the human connectome project. *Eur. J. Neurosci.* 45, 1224–1229. <https://doi.org/10.1111/ejn.13544>.
- Trevisan, N., Miola, A., Cattarinussi, G., Kubera, K.M., Hirjak, D., Wolf, R.C., Sambataro, F., 2022. Cortical folding complexity is distinctively altered in schizophrenia and bipolar disorder. *Schizophr. Res.* 241, 92–93. <https://doi.org/10.1016/j.schres.2022.01.037>.
- Turner, J.A., Damaraju, E., van Erp, T.G.M., Mathalon, D.H., Ford, J.M., Voyvodic, J., Mueller, B.A., Belger, A., Bustillo, J., McEwen, S., Potkin, S.G., Calhoun, V.D., 2013. A multi-site resting state fMRI study on the amplitude of low frequency fluctuations in schizophrenia. *Front. Neurosci.* 7. <https://doi.org/10.3389/FNINS.2013.00137>.
- Uhlhaas, P.J., Singer, W., 2010. Abnormal neural oscillations and synchrony in schizophrenia. *Nat. Rev. Neurosci.* <https://doi.org/10.1038/nrn2774>.
- van Leeuwen, J.M.C., Vinkers, C.H., Vink, M., Kahn, R.S., Joëls, M., Hermans, E.J., 2021. Disrupted upregulation of salience network connectivity during acute stress in siblings of schizophrenia patients. *Psychol. Med.* 51, 1038–1048. <https://doi.org/10.1017/S0033291719004033>.
- Vanhatalo, S., Palva, J.M., Holmes, M.D., Miller, J.W., Voipio, J., Kaila, K., 2004. Infraslow oscillations modulate excitability and interictal epileptic activity in the human cortex during sleep. *Proc. Natl. Acad. Sci. U. S. A.* 101, 5053–5057. <https://doi.org/10.1073/pnas.0305375101>.
- Wang, Z., Li, Y., Childress, A.R., Detre, J.A., 2014. Brain entropy mapping using fMRI. *PLoS One* 9, e89948. <https://doi.org/10.1371/journal.pone.0089948>.
- Wang, X., Zhang, W., Sun, Y., Hu, M., Chen, A., 2016. Aberrant intra-salience network dynamic functional connectivity impairs large-scale network interactions in schizophrenia. *Neuropsychologia* 93, 262–270. <https://doi.org/10.1016/j.neuropsychologia.2016.11.003>.
- Wang, J., Wang, Y., Huang, H., Jia, Y., Zheng, S., Zhong, S., Huang, L., Huang, R., 2019a. Abnormal intrinsic brain functional network dynamics in unmedicated depressed bipolar II disorder. *J. Affect. Disord.* 253, 402–409. <https://doi.org/10.1016/j.jad.2019.04.103>.
- Wang, X., Liao, W., Han, S., Li, J., Zhang, Y., Zhao, J., Chen, H., 2019b. Altered dynamic global signal topography in antipsychotic-naïve adolescents with early-onset schizophrenia. *Schizophr. Res.* 208, 308–316. <https://doi.org/10.1016/j.schres.2019.01.035>.
- Wang, J., Wang, Y., Huang, H., Jia, Y., Zheng, S., Zhong, S., Chen, G., Huang, L., Huang, R., 2020. Abnormal dynamic functional network connectivity in unmedicated bipolar and major depressive disorders based on the triple-network model. *Psychol. Med.* 50, 465–474. <https://doi.org/10.1017/S003329171900028X>.
- Wang, Y., Jiang, Y., Collin, G., Liu, D., Su, W., Xu, L., Wei, Y., Tang, Y., Zhang, T., Tang, X., Hu, Y., Zhang, J., Cui, H., Wang, Jinhong, Yao, D., Luo, C., Wang, Jijun, 2021. The effects of antipsychotics on interactions of dynamic functional connectivity in the triple-network in first episode schizophrenia. *Schizophr. Res.* 236, 29–37. <https://doi.org/10.1016/j.schres.2021.07.038>.
- Watson, D., Clark, L.A., Tellegen, A., 1988. Development and validation of brief measures of positive and negative affect: the PANAS scales. *J. Pers. Soc. Psychol.* 54, 1063–1070. <https://doi.org/10.1037/0022-3514.54.6.1063>.
- Weber, S., Johnsen, E., Kroken, R.A., Løberg, E.M., Kandilarova, S., Stoyanov, D., Kompus, K., Høgdahl, K., 2020. Dynamic functional connectivity patterns in schizophrenia and the relationship with hallucinations. *Front Psychiatry* 11. <https://doi.org/10.3389/fpsy.2020.00227>.
- Wen, L., Liu, S., Cao, Y., Li, G., 2019. Construction and Recognition of Functional Brain Network Model Based on Depression. *J. Med. Syst.* 43 (8), 1–8. <https://doi.org/10.1007/S10916-019-1198-4>.
- Whitfield-Gabrieli, S., Ford, J.M., 2012. Default mode network activity and connectivity in psychopathology. *Annu. Rev. Clin. Psychol.* <https://doi.org/10.1146/annurev-clinpsy-032511-143049>.
- Wu, D., Jiang, T., 2020. Schizophrenia-related abnormalities in the triple network: a meta-analysis of working memory studies. *Brain Imag. Behav.* 14, 971–980. <https://doi.org/10.1007/S11682-019-00071-1>.
- Wu, L., Caprihan, A., Bustillo, J., Mayer, A., Calhoun, V., 2018. An approach to directly link ICA and seed-based functional connectivity: application to schizophrenia. *Neuroimage* 179, 448. <https://doi.org/10.1016/j.neuroimage.2018.06.024>.
- Xi, C., Liu, Z., Ning, Yang, J., Zhang, W., Deng, M., Jie, Pan, Y., Zhi, Cheng, Y., Qi, Pu, W., Dan, 2020. Schizophrenia patients and their healthy siblings share decreased prefronto-thalamic connectivity but not increased sensorimotor-thalamic connectivity. *Schizophr. Res.* 222, 354–361. <https://doi.org/10.1016/J.SCHRES.2020.04.033>.
- Yang, G.J., Murray, J.D., Repovs, G., Cole, M.W., Savic, A., Glasser, M.F., Pittenger, C., Krystal, J.H., Wang, X.J., Pearson, G.D., Glahn, D.C., Anticevic, A., 2014. Altered global brain signal in schizophrenia. *Proc. Natl. Acad. Sci. U. S. A.* 111, 7438–7443. <https://doi.org/10.1073/PNAS.1405289111/-DCSUPPLEMENTAL/PNAS.1405289111.SAPP.PDF>.
- Yang, Y., Qian, C., Huafu, C., 2020. Altered inter-hemispheric functional connectivity dynamics in bipolar disorder. In: 2020 17th International Computer Conference on Wavelet Active Media Technology and Information Processing (ICCWAMTIP). [https://doi.org/10.1109/ICCWAMTIP51612.2020.9317369/20/\\$31.00](https://doi.org/10.1109/ICCWAMTIP51612.2020.9317369/20/$31.00).
- Yang, W., Xu, X., Wang, C., Cheng, Y., Li, Y., Xu, S., Li, J., 2022. Alterations of dynamic functional connectivity between visual and executive-control networks in schizophrenia. *Brain Imag. Behav.* 16, 1294–1302. <https://doi.org/10.1007/s11682-021-00592-8>.
- Young, R.C., Biggs, J.T., Ziegler, V.E., Meyer, D.A., 1978. A rating scale for mania: reliability, validity and sensitivity. *Br. J. Psychiatry* 133, 429–435. <https://doi.org/10.1192/BJP.133.5.429>.
- Yu, Q., Allen, E., Sui, J., Arbabshirani, R., Pearson, G., Calhoun, V.D., 2013. Brain connectivity networks in schizophrenia underlying resting State functional magnetic resonance imaging. *Curr. Top. Med. Chem.* 12, 2415–2425. <https://doi.org/10.2174/156802612805289890>.
- Yue, J.L., Li, P., Shi, L., Lin, X., Sun, H.Q., Lu, L., 2018. Enhanced temporal variability of amygdala-frontal functional connectivity in patients with schizophrenia. *Neuroimage Clin.* 18, 527–532. <https://doi.org/10.1016/j.nicl.2018.02.025>.

- Zang, Y., Jiang, T., Lu, Y., He, Y., Tian, L., 2004. Regional homogeneity approach to fMRI data analysis. *NeuroImage* 22 (1), 394–400. <https://doi.org/10.1016/J.NEUROIMAGE.2003.12.030>.
- Zarghami, T.S., Hossein-Zadeh, G.A., Bahrami, F., 2020. Deep temporal organization of fMRI phase synchrony modes promotes large-scale disconnection in schizophrenia. *Front. Neurosci.* 14 <https://doi.org/10.3389/fnins.2020.00214>.
- Zhang, J., Northoff, G., 2022. Beyond noise to function: reframing the global brain activity and its dynamic topography. *Commun. Biol.* 5 <https://doi.org/10.1038/S42003-022-04297-6>.
- Zhang, J., Cheng, W., Liu, Z., Zhang, K., Lei, X., Yao, Y., Becker, B., Liu, Y., Kendrick, K. M., Lu, G., Feng, J., 2016. Neural, electrophysiological and anatomical basis of brain-network variability and its characteristic changes in mental disorders. *Brain* 139, 2307–2321. <https://doi.org/10.1093/brain/aww143>.
- Zhang, Z., Zhuo, K., Xiang, Q., Sun, Yi, Suckling, J., Wang, J., Liu, D., Sun, Yu, 2021. Dynamic functional connectivity and its anatomical substrate reveal treatment outcome in first-episode drug-naïve schizophrenia. *Transl. Psychiatry* 11. <https://doi.org/10.1038/s41398-021-01398-4>.
- Zhu, J., Zhang, S., Cai, H., Wang, C., Yu, Y., 2020. Common and distinct functional stability abnormalities across three major psychiatric disorders. *Neuroimage Clin.* 27 <https://doi.org/10.1016/j.nicl.2020.102352>.